

N-heterocyclic carbene adducts of the heavier group 15 tribromides. Normal to abnormal isomerism and bromide ion abstraction.

*Jordan B. Waters, Qien Chen, Thomas A. Everitt and Jose M. Goicoechea**

Department of Chemistry, University of Oxford, Chemistry Research Laboratory,

12 Mansfield Road, Oxford, OX1 3TA, U.K.

E-mail: jose.goicoechea@chem.ox.ac.uk

Abstract

The reactivity of the heavier group 15 tribromides, SbBr₃ and BiBr₃, towards 1,3-bis(2,6-diisopropylphenyl)-imidazol-2-ylidene (IPr) is described. These reactions quantitatively afford Lewis acid–base adducts, (IPr)EBr₃ (E = Sb (**1**), Bi (**2**)), which readily react with AlBr₃ yielding cationic species [(IPr)EBr₂]⁺ (E = Sb (**3**), Bi (**4**)). Under thermal treatment, the N-heterocyclic carbene ligands in **1** and **2** will readily isomerise to afford the abnormally-bonded (or mesoionic) complexes (aIPr)EBr₃ (E = Sb (**5**), Bi (**6**)). As with **1** and **2**, bromide abstraction from such compounds readily affords the cationic complexes [(aIPr)EBr₂]⁺ (E = Sb (**7**), Bi (**8**)). Finally, in an effort to elucidate the isomerisation process which allows for the conversion of **1** and **2** to the abnormally bonded systems (compounds **5** and **6**), compound **1** was reacted with a further equivalent of IPr to afford the cationic species [(aIPr)₂SbBr₂]⁺ (**9**). This strongly suggests that the normal to abnormal isomerisation of the N-heterocyclic carbene ligands in compounds **1** and **2** is mediated by the presence of free IPr. Compound [**9**]Br can be used to access the dicationic species [(aIPr)₂SbBr]²⁺ (**10**), which we have identified spectroscopically. Single crystal X-ray structures and spectroscopic data for all compounds are discussed.

1. Introduction

Over the course of the last 25 years, N-heterocyclic carbenes (NHCs) have become one of the most versatile family of ligands available in coordination chemistry.^[1–12] Their strong σ -donor properties, and tuneable steric profiles, make them attractive supports for a range of Lewis acidic metal and non-metal compounds. Of all of the known isolable carbenes, arguably the most commonly utilized are imidazol-2-ylidenes which have an unsaturated ligand backbone and are known to exhibit isomerism on bonding to metal centres.^[13] Such species most commonly bond to Lewis acidic compounds via the carbenic C2 position (in the so-called “normal” bonding mode). However it is also possible for proton migration to occur between the alkenic backbone and the carbene centre, allowing these ligands to coordinate via the backbone C4/C5 position (in what is termed an “abnormal” or “mesoionic” bonding mode).

In main group chemistry, imidazol-2-ylidenes have been extensively employed for the isolation of low coordinate, low oxidation state compounds, such as $E_2(\text{NHC})_2$ ($E = \text{B}, \text{Si}–\text{Sn}, \text{P}, \text{As}$).^[14–21] More recently, related cyclic alkylamino carbenes (CAACs) have also been employed to access base-stabilized diatomic molecules $E_2(\text{CAAC})_2$ ($E = \text{B}, \text{Si}, \text{P}, \text{Sb}$).^[22–25] Such species are typically accessed by the chemical reduction of carbene-stabilized main group element halide precursors $(\text{NHC})\text{EX}_n$ ($n = 2–4$) with strong reductants. Consequently Lewis acid–base adducts of N-heterocyclic carbenes with group 13 trihalides, group 14 di- and tetrahalides, and group 15 trihalides have been extensively studied. Of all of these adducts, those between main group element bromides and N-heterocyclic carbenes are amongst the least extensively studied. We recently reported that coordination of 1,3-bis(2,6-diisopropylphenyl)-imidazol-2-ylidene (IPr) to PBr_3 results in the initial formation of a 1:1 adduct, $(\text{IPr})\text{PBr}_3$, which on thermal treatment evolves bromine gas (Br_2) in a carbene

induced reductive coupling of phosphorus to yield the ionic compound $[P_2(IPr)_2Br_3]Br$.^[26] Herein we expand these studies to the heavier group 15 tribromides, $SbBr_3$ and $BiBr_3$, and show that thermal treatment of the 1:1 adducts $(IPr)EBr_3$ ($E = Sb$ (**1**), Bi (**2**)) does not result in the reductive coupling of the main group elements, but rather in a normal-to-abnormal isomerisation of the coordination mode of the carbene to afford $(aIPr)EBr_3$ ($E = Sb$ (**5**), Bi (**6**)).

2. Results and discussion

2.1. Synthesis of *IPr* adducts with EBr_3 ($E = Sb$, **1**; Bi , **2**)

Addition of one molar equivalent of EBr_3 ($E = Sb, Bi$) to a diethyl ether solution of *IPr* results in the formation of the 1:1 Lewis acid–base adducts $(IPr)EBr_3$ ($E = Sb$ (**1**), Bi (**2**)). Both **1** and **2** instantaneously precipitate from the reaction mixtures upon mixing of the reagents and can be isolated as pale (**1**) and bright yellow (**2**) solids in high yields. Compounds **1** and **2** were characterised by 1H and $^{13}C\{^1H\}$ NMR spectroscopy in d_8 -THF revealing the presence of a symmetric 1,3-bis(2,6-diisopropylphenyl)-imidazol-2-ylidene (*IPr*) ligand. The most diagnostic resonances in the 1H NMR spectra are those of the imidazol-2-ylidene backbone, which are observed as singlets at 7.92 and 7.79 ppm, and the methine resonances of the diisopropylphenyl functionalities which are observed at 3.21 and 3.16 ppm for **1** and **2**, respectively. The carbene ^{13}C NMR resonances were observed at 156.2 for **1** and 194.9 ppm for **2**. The latter of these is significantly broadened due to coupling to the 100% abundant, quadrupolar ($I = 9/2$) ^{209}Bi nucleus.^[27]

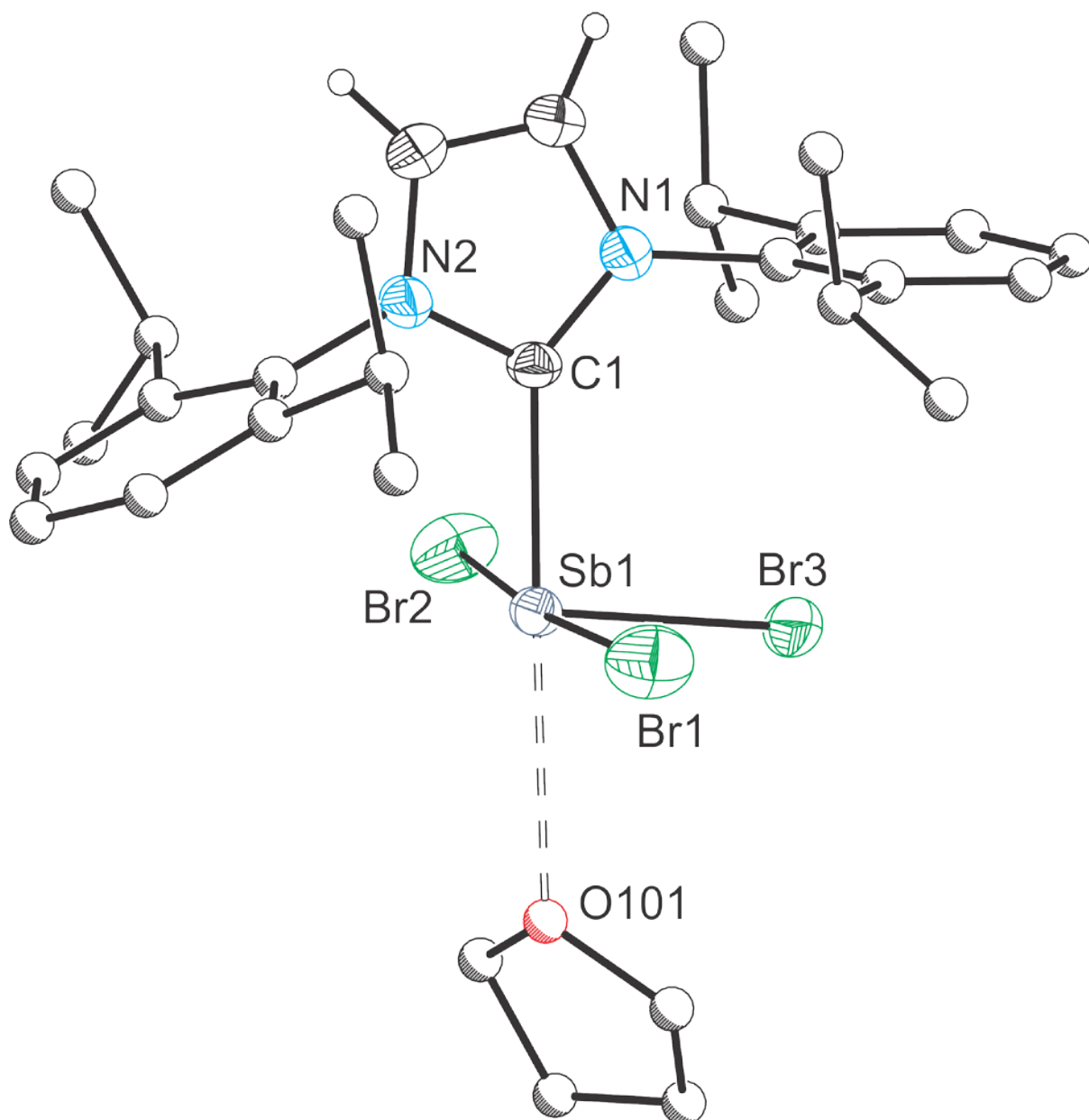


Figure 1. Molecular structure of **1·2THF** (major component of the positionally disordered molecule pictured). Anisotropic displacement ellipsoids pictured are set at 50% probability. Hydrogen atoms (with the exception of the imidazole protons) and one of the two crystallographically independent THF molecules have been omitted for clarity. Atoms of the Dipp groups, the THF molecule, and hydrogen atoms are pictured as spheres of arbitrary radii. Selected bond distances (Å) and angles (°): Sb1–Br1, 2.727(1); Sb1–Br2, 2.729(1); Sb1–Br3, 2.508(1); Sb1–C1, 2.268(3); Sb1···O101, 2.904(3). Br1–Sb1–Br2, 173.32(2); Br1–Sb1–Br3, 87.46(2); Br1–Sb1–C1, 93.27(9); Br1–Sb1–O101, 91.81(7); Br2–Sb1–Br3,

86.52(2); Br2–Sb1–C1, 84.54(9); Br2–Sb1–O101, 90.04(7); Br3–Sb1–C1, 96.27(9); Br3–Sb1–O101, 80.60(8); C1–Sb1–O101, 173.92(12).

Single crystals of **1**·2THF were grown from a saturated THF solution of **1** at –25 °C. Analysis of the molecular structure reveals a disphenoidal (see-saw) geometry about the antimony centre with respect to the IPr and bromine ligands (Figure 1). However, there is also a close contact observed between the antimony centre and one of the two crystallographically independent THF molecules. The coordinated solvent molecule adopts a *trans* arrangement to the IPr ligand, resulting in a five coordinate antimony centre with a square based pyramidal geometry. The second THF molecule is uncoordinated and shows no close contacts with **1**. The geometry can be described by the τ_5 parameter which is 0.010,^[28] in line with what would be expected of a true square based pyramidal geometry. The close contact observed with the THF molecule in the solid state can be explained by the increase in Lewis acidity of the group 15 centre when compared to (IPr)PBr₃. The reduction in hybridisation of s and p orbitals results in the lone pair of electrons occupying an orbital of greater s character (hence the reduced basicity and stereochemical influence) whilst bonding orbitals are formed using a greater contribution from the p orbitals. Therefore, donation of a pair of electrons from a coordinating THF molecule into the σ^* of the Sb–C bond becomes a favourable interaction. The antimony lone pair of electrons is likely directed towards a position *trans* to Br3. The Sb1–O101 distance of 2.904(3) Å is significantly greater than that of a two-centre-two-electron Sb–O covalent bond ($\Sigma r_{\text{cov}} = 2.05$ Å).^[29] However, this distance is shorter than the sum of van der Waals radii of antimony and oxygen (3.35 Å) hence a weak bonding interaction is clearly present.^[30]

The Sb1–C1 bond length (2.268(3) Å) is approximately 0.40 Å longer than the P–C bond present in the previously reported (IPr)PBr₃,^[25] which is marginally longer than expected based on the larger covalent radius of antimony compared to arsenic ($\Delta r_{\text{cov}} = 0.32$ Å). This may be due to the donation of electron density into the Sb–C σ^* orbital by the THF molecule reducing the IPr–Sb bonding interaction. There are no other structurally authenticated imidazol-2-ylidene adducts of antimony trihalides reported in the chemical literature for bond metric comparison. That being said, an adduct of SbCl₃ with the expanded ring carbene :C[N(Dipp)CH₂]₂CH₂ (Dipp = 2,6-diisopropylphenyl) has been reported and shown to have comparable bond metrics ($d_{\text{Sb–C}} = 2.288(2)$ Å).^[31]

The hypervalent nature of the antimony centre is evident in the Sb–Br bond lengths which are notably longer for the axial bromine atoms (2.727(1) and 2.729(1) Å) than that observed for the equatorial Sb1–Br3 bond length (2.508(1) Å). The linear Br1–Sb1–Br2 moiety can be described as a three-centre, four-electron bond, as a result of the donation of the carbene lone pair of electrons into a Sb–Br σ^* orbital which explains the significantly longer Sb–Br bond lengths (Figure 2).^[32] The latter Sb1–Br3 bond length is within the range expected based on the sum of covalent radii ($\Sigma r_{\text{cov}} = 2.59$ Å).

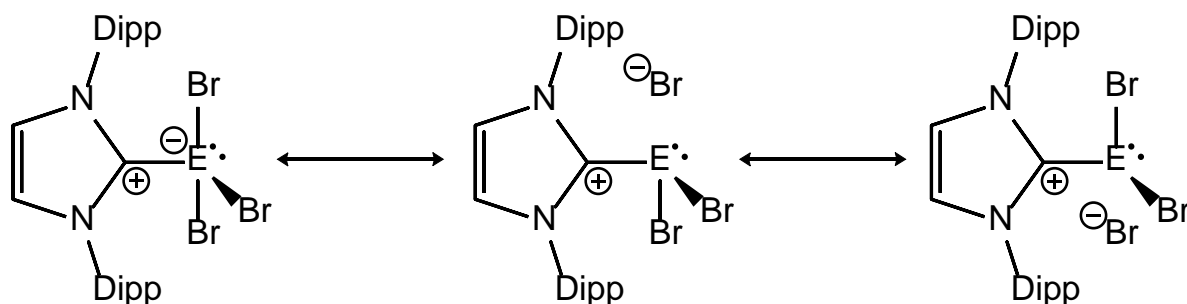


Figure 2. Different resonance structures for (IPr)EBr₃.

Bright yellow crystals of (IPr)BiBr₃·0.5THF (**2**·0.5THF) suitable for single crystal X-ray diffraction were grown by slow diffusion of hexane into a THF solution of **2**. The structure of

2 differs significantly from that of **1**. Two molecules of **2** dimerise through weak interactions in the lattice to afford $[(\text{IPr})\text{BiBr}_2(\mu\text{-Br})_2]_2$, a result of donation of electron density from an apical bromine atom of one molecule into the σ^* of the Bi–C bond of another molecule, resulting in the formation of two bromide bridges (Figure 3). The square based pyramidal geometry about both Bi1 and Bi2 can be quantified by the τ_5 parameter which was calculated as 0.091 and 0.198, respectively. The molecular structure does not contain any symmetry elements as a result of the butterfly shape afforded by the Bi1–Br3–Bi2–Br6 ring.

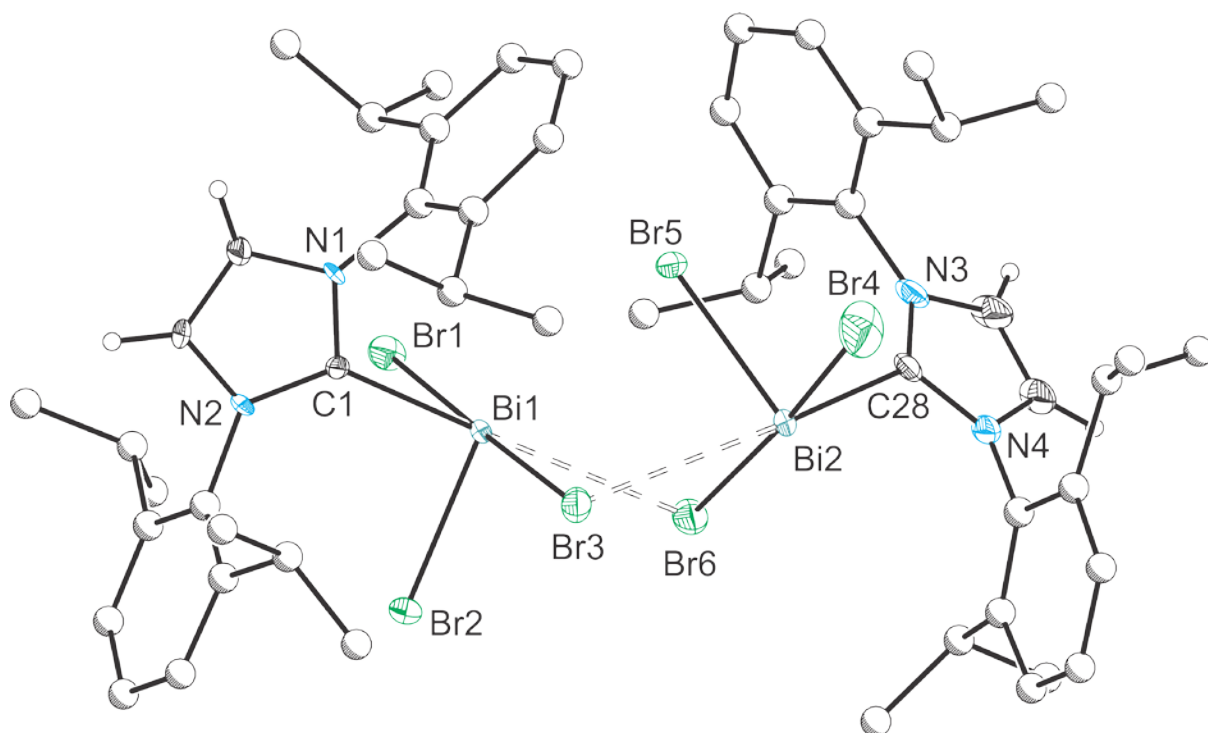


Figure 3. Molecular structure of one of the two crystallographically independent dimeric units of **2**. Anisotropic displacement ellipsoids pictured are set at 50% probability. Hydrogen atoms (with the exception of the imidazole protons) have been omitted for clarity. Atoms of the Dipp groups and hydrogen atoms are pictured as spheres of arbitrary radii. Selected bond distances (Å) and angles (°): Bi1–Br1, 2.792(1); Bi1–Br2, 2.619(1); Bi1–Br3, 2.850(1); Bi1–C1, 2.418(6); Bi1···Br5, 3.3890(7); Bi1···Br6, 3.255(1); Bi2–Br4, 2.759(1); Bi2–Br5, 2.606(1); Bi2–Br6, 2.855(1); Bi2–C28, 2.400(7); Bi2···Br3, 3.287(1). Br1–Bi1–Br2, 90.79(2); Br1–Bi1–Br3, 178.01(2); Br1–Bi1–C1, 86.19(14); Br1–Bi1–Br6, 100.66(2); Br2–

Bi1–Br3, 90.89(3); Br2–Bi1–C1, 96.43(14); Br2–Bi1–Br6, 86.42(2); Br3–Bi1–C1, 92.55(14); Br3–Bi1–Br6, 80.53(2); C1–Bi1–Br6, 172.57(14); Br4–Bi2–Br5, 89.09(3); Br4–Bi2–Br6, 175.38(3); Br4–Bi2–C28, 99.13(16); Br4–Bi2–Br3, 95.99(3); Br5–Bi2–Br6, 88.21(2); Br5–Bi2–C28, 92.32(17); Br5–Bi2–Br3, 81.33(2); Br6–Bi2–C28, 84.73(16); Br6–Bi2–Br3, 79.90(2); Br3–Bi2–C28, 163.50(17); Bi1–Br3–Bi2, 84.40(2); Bi1–Br6–Bi2, 84.91(2).

The angles within the Bi₂Br₂ core are all smaller than 90° which results in a buckling of the ring ($\Sigma_{\text{internal angles}} = 329.7^\circ$). This is in contrast to the molecular structure observed for [(IPr)BiCl₂(μ -Cl)]₂ in which the Bi₂Cl₂ moiety is planar and there is a centre of inversion.^[32] The only apparent reason for the structural distortion from a planar geometry is a result of the close contact observed between Bi1 and Br5. The distance at 3.389(1) Å is significantly greater than the sum of covalent radii for bismuth and bromine (2.68 Å) however, is within the sum of van der Waals radii (3.70 Å) which is evidence of a bonding interaction. The Bi1–C1 and Bi2–C28 bond lengths are very similar at 2.418(6) and 2.400(7) Å, and are consistent with that observed for the only other structurally characterised (NHC)BiX₃ species, [(IPr)BiCl₂(μ -Cl)]₂, which has a Bi–C bond length of 2.389(8) Å.^[33]

As is observed for (IPr)PBr₃ and **1**, the ‘axial’ bromine atoms (Br1, Br3, Br4 and Br6) have a notably longer bond length to the bismuth atoms than the ‘equatorial’ bromine atoms (Br2 and Br5). Additionally, the Bi1–Br3 and Bi2–Br6 are slightly lengthened (2.850(1) and 2.855(1) Å, respectively) relative to the other axial bond (Bi1–Br1 (2.792(1) Å) and Bi2–Br4 (2.759(1) Å), respectively) as a result of dimerisation and donation of electron density from the bromine atoms into the σ^* of the opposite Bi–C bond. As expected, the ‘equatorial’ Bi1–Br2 and Bi2–Br5 bond lengths (2.619(1) and 2.606(1) Å, respectively) are within the range

expected for a covalent Bi–Br single bond. Finally, the distances between the bridging bromine atoms and that of the opposite bismuth centre are significantly longer than all other Bi–Br bond lengths. The Bi1–Br6 and Bi2–Br3 interatomic distances are 3.255(1) and 3.287(1) Å, respectively, and, while long, are still within the sum of van der Waals radii for bismuth and bromine.

2.2. Bromide abstraction from **1** and **2**

The formation of an adduct between EBr₃ and the strong two electron sigma donor, IPr, results in a weakening of the E–Br bonds (Figure 2). The steric bulk of the IPr ligand also reduces the nucleophilicity of the element centre, hence, we sought to abstract one of the coordinating bromide ligands with the use of the highly Lewis acidic reagent, AlBr₃, thereby generating an [AlBr₄][–] counter anion. Indeed, addition of one equivalent of AlBr₃ to **1** and **2** allows for the synthesis of [(IPr)EBr₂][AlBr₄] (E = Sb, [**3**][AlBr₄]; Bi, [**4**][AlBr₄]). The reaction must be carried out in a non-coordinating solvent, and we found that dichloromethane was an ideal choice for such experiments. Both products can be isolated in greater than 79% yield and crude NMR spectra reveal quantitative formation of the cationic species. Analysis of crystalline samples by ¹H and ¹³C{¹H} NMR spectroscopy in CD₂Cl₂ reveals a symmetric IPr ligand with a change in the chemical shift of the resonances indicating the formation of the cationic species **3** and **4**.

The ¹H NMR spectra of **3** and **4** reveal an upfield shift of the imidazol-2-ylidene backbone protons upon bromide ion abstraction to 7.78 and 7.69 ppm, respectively (cf. 7.92 and 7.79 ppm for **1** and **2**, respectively). The same effect is also observed to the methine resonances of the diisopropylphenyl groups which were observed at 2.50 ppm for **3** and 2.55 ppm for **4** (cf. 3.21 and 3.16 ppm for **1** and **2**, respectively).

The ^{13}C NMR chemical shift of the carbene resonances are also shifted upfield relative to that of the starting materials for **3** and **4** ($\Delta\delta = 5.9$ and 3.6 ppm, respectively). The reduction in the difference in chemical shifts ($\Delta\delta$) of the carbene resonance between **3** and **4** is consistent with the weaker bonding interaction between the carbene carbon and the heavier (and larger) group 15 element. This also has the effect of a general downfield shift of the carbene resonance in both sets of **1–2** and **3–4** due to the greater carbenic character retained by the ligand due to poorer orbital overlap with the heavier elements. Solutions of [**3**][AlBr₄] and [**4**][AlBr₄] also give rise to a relatively sharp singlet resonance in the ^{27}Al NMR spectrum at 80.9 and 81.1 ppm, respectively, which results from the tetrahedral [AlBr₄][–] anion.

Additional evidence for the formation of the cationic species comes from analysis by positive-ion mode electrospray ionisation mass-spectrometry (ESI-MS) which reveals a single mass envelope that can be ascribed to the molecular ion for each sample in dichloromethane. Analysis of [**3**][AlBr₄] and [**4**][AlBr₄] reveals a mass envelope at 669.1093 for [(IPr)SbBr₂]⁺ (Calcd 669.0266) and 757.1798 for [(IPr)BiBr₂]⁺ (Calcd 757.1025), respectively.

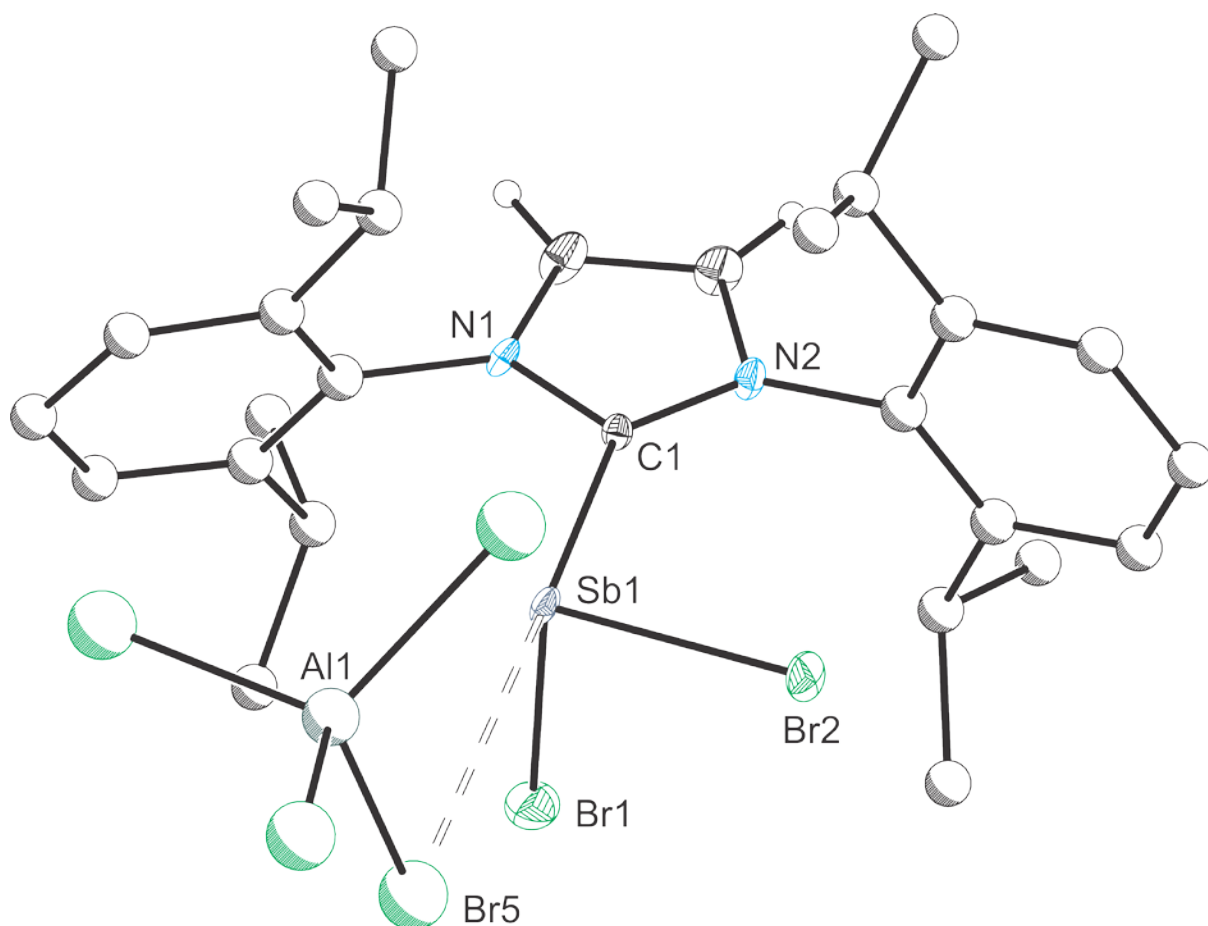


Figure 4. Structure of one of the two crystallographically independent units of **[3][AlBr₄]**. Anisotropic displacement ellipsoids pictured are set at 50% probability. Hydrogen atoms (with the exception of the imidazole protons) and solvent of crystallisation have been omitted for clarity. Atoms of the Dipp groups, the tetrabromoaluminate anion and hydrogen atoms are pictured as spheres of arbitrary radii. Sb1–Br1, 2.499(1); Sb1–Br2 2.488(1); Sb1–C1, 2.223(4); Sb1···Br5, 3.412(1). Br1–Sb1–Br2, 96.13(2); Br1–Sb1–C1, 89.82(9); Br1–Sb1–Br5, 83.98(2); Br2–Sb1–C1, 97.76(10); Br2–Sb1–Br5, 85.92(2); Br5–Sb1–C1, 173.11(10).

Colourless and pale yellow crystals of **[3][AlBr₄]**·0.5CH₂Cl₂ and **[4][AlBr₄]**·0.5CH₂Cl₂ were grown by slow diffusion of hexane into dichloromethane solution of **3** and **4**, respectively. Analysis of the structure of **3** (Figure 4) reveals a trigonal pyramidal geometry about the antimony centre. An additional close contact between the antimony and a bromide ligand of

the $[\text{AlBr}_4]^-$ anion is present in the solid state giving rise to a four-coordinate antimony centre in a distorted, disphenoidal geometry which can be quantified by the τ_4' parameter (0.396).^[34] This value is notably closer to the optimal value for a disphenonidal structure (0.24) relative to a tetrahedral one (1). The bromide of the counter anion lies *trans* to the IPr ligand by donation of electron density into the σ^* of the Sb–C bond (as opposed to the σ^* of either Sb–Br bonds). In all likelihood, this results from the increased steric bulk of the tetrabromoaluminate anion when compared to the bromide ion itself and this prevents coordination *trans* to a bound bromide ligand. Correspondingly, the Sb–Br distance is quite long at 3.412(1) Å, but shorter than the calculated value for the sum of van der Waals radii (3.65 Å).^[30] It should be noted that these distances are strongly dependant on crystal packing effects and that the other crystallographically unique molecule of **3** present in the asymmetric unit exhibits much longer interactions between the antimony centre and the bromine atoms of the nearest adjacent tetrabromoaluminate anion (3.657(1) and 3.686(1) Å). These latter fall just outside the sum of Van der Waals radii and highlight the weak nature of such interactions.

The structure of **4** also reveals a close contact between the bismuth atom and a bromide ligand of the $[\text{AlBr}_4]^-$ anion (Figure 5). This gives rise to a four-coordinate centre with a distorted disphenoidal geometry which can be quantified by the τ_4' parameter (0.397). Again, the distance from the group 15 element to the bromide ligand of the tetrabromoaluminate anion is long at 3.354(1) Å, however within the sum of van der Waals radii for bismuth and bromine (3.70 Å).

The Sb1–C1 and Bi1–C1 bond distances of 2.223(4) and 2.355(5) Å, observed for **3** and **4**, respectively, are slightly shorter than those observed for **1** and **2**, consistent with increased

bonding character between the ligand and the group 15 element upon bromide abstraction. The same effect is also observed for the bond lengths to the bonded bromine atoms. The Sb1–Br1 and Sb1–Br2 bond lengths in **3** and Bi1–Br1 and Bi1–Br2 bond lengths in **4** are shorter at 2.499(1) and 2.488(1) Å, and 2.589(1) and 2.574(1) Å, respectively, when compared to the neutral precursors (**1** and **2**). Finally, a reduction in the C–E–Br bond angles was also observed upon changing Sb (89.82(9) and 97.76(10)°) to Bi (89.16(11) and 96.98(12)°) as a result of the reduced hybridisation between s and p orbitals and increased contribution from the element p orbitals in bonding.

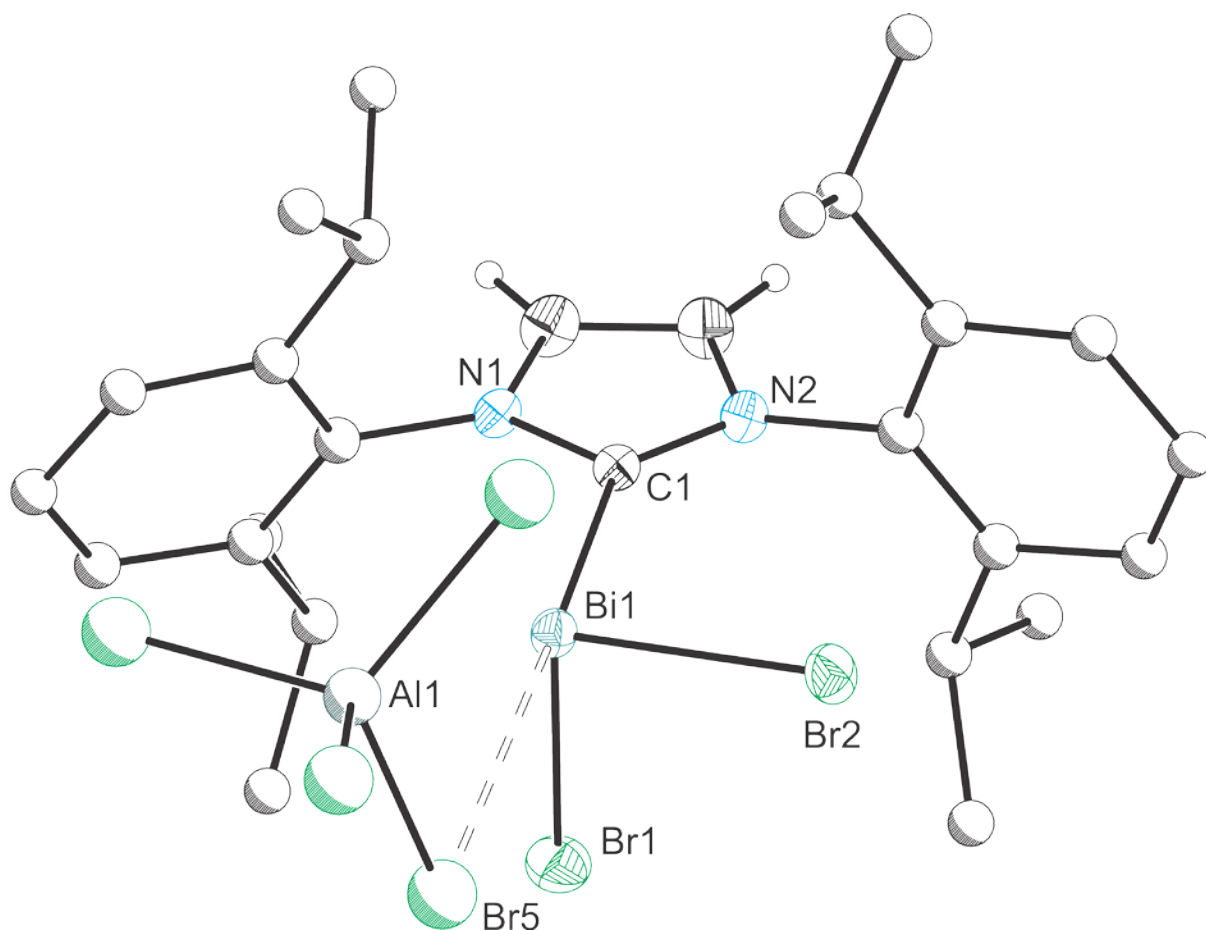
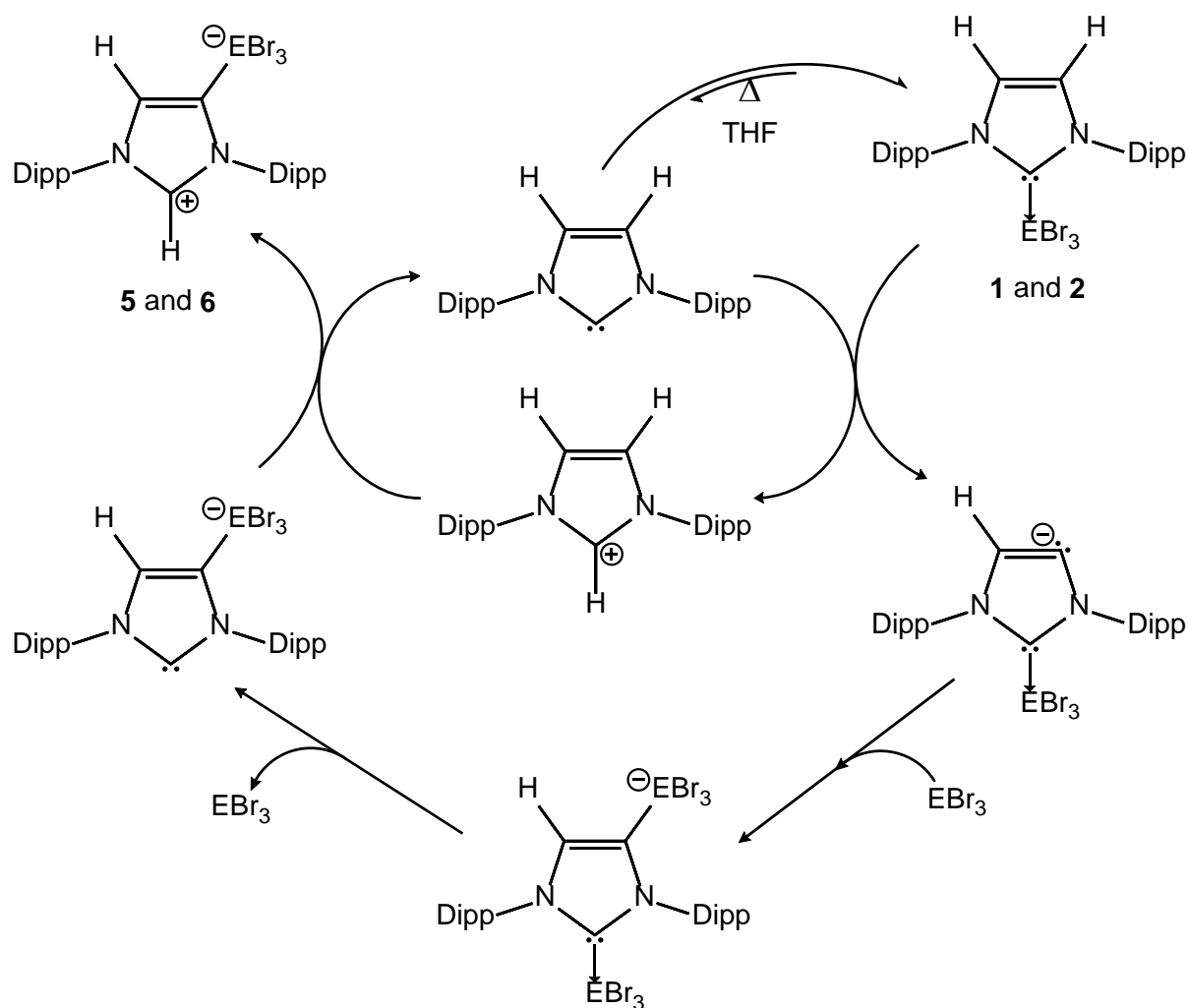


Figure 5. Structure of one of the two crystallographically independent units of **[4][AlBr₄]**. Anisotropic displacement ellipsoids pictured are set at 50% probability. Hydrogen atoms (with the exception of the imidazole protons) and solvent of crystallisation have been omitted for clarity. Atoms of the Dipp groups, the tetrabromoaluminate anion and hydrogen atoms are

pictured as spheres of arbitrary radii. Bi1–Br1, 2.589(1); Bi1–Br2 2.574(1); Bi1–C1, 2.355(5); Bi1...Br5, 3.354(1). Br1–Bi1–Br2, 95.32(2); Br1–Bi1–C1, 89.16(11); Br1–Bi1–Br5, 85.15(2); Br2–Bi1–C1, 96.98(12); Br2–Bi1–Br5, 87.14(2); C1–Bi1–Br5, 173.27(11).

2.3. Isomerisation of IPr in **1** and **2** to afford (aIPr)EBr₃ (E = Sb, **5**; Bi, **6**)

During the synthesis of (IPr)EBr₃ it is vital that there be no excess of IPr in solution for an extended period of time. The presence of excess IPr allows for the isomerisation of the coordinated IPr ligand via a proton shuttling mechanism. Carrying out the reaction of IPr with SbBr₃ or BiBr₃ in diethyl ether allows for the precipitation and isolation of **1** and **2** in high yield. Conversely, if the reaction is carried out in THF, it is possible to observe isomerised products along with small amounts of [IPrH]Br. Ultimately, it was determined that heating a THF solution of analytically pure **1** or **2** (obtained as precipitates from diethyl ether) at 75 °C allows for the isomerisation of the IPr ligand affording (aIPr)SbBr₃ (**5**) after three days and (aIPr)BiBr₃ (**6**) after one day in essentially quantitative yields (when the reaction was carried out and monitored in *d*₈-THF). These compounds can be isolated in greater than 60% crystalline yields upon diffusion of hexane into the reaction mixtures. This reaction likely proceeds via the cleavage of the E–C bond generating free IPr in solution, which upon heating allows for the facile deprotonation of a coordinated IPr ligand which has increased in acidity due to the inductively electron withdrawing EBr₃ group. A general proposed mechanism is given in Scheme 1 which clearly illustrates the catalytic nature of IPr in the transformation.



Scheme 1. Proposed mechanism for the isomerisation of IPr coordinated to group 15 tribromides upon heating in THF thereby generating **5** and **6**.

Isomerisation results in an asymmetric ligand environment and a concomitant doubling of a number of the resonances in the ^1H and $^{13}\text{C}\{^1\text{H}\}$ NMR spectra. This is clearly evidenced by the appearance of two septet resonances in the methine region of the spectrum arising from the inequivalent Dipp functionalities (3.06 and 2.64 ppm for **5** and 3.00 and 2.57 ppm for **6**). Diagnostically, the presence of a downfield doublet resonance arising from the imidazolium proton bonded to the C2 carbon indicates isomerisation of the ligand (observed at 9.37 and 9.36 ppm for **5** and **6**, respectively), along with a second doublet resonance of equal intensity arising from the remaining alkenic imidazole proton (at 8.37 and 8.46 ppm, respectively).

The C4 bonded carbanionic position was observed at 148.4 and 191.8 ppm in the ^{13}C NMR spectrum for **4** and **5**, respectively.

Single crystals of both abnormal complexes of antimony tribromide and bismuth tribromide, **5** and **6** respectively, were grown by slow diffusion of hexane into THF solutions of the products. Analysis of the molecular structure reveals a dimeric structure of the form $[(\text{aIPr})\text{EBr}_2(\mu\text{-Br})]_2$ which contains two bridging bromide ligands (Figures 6 and 7).

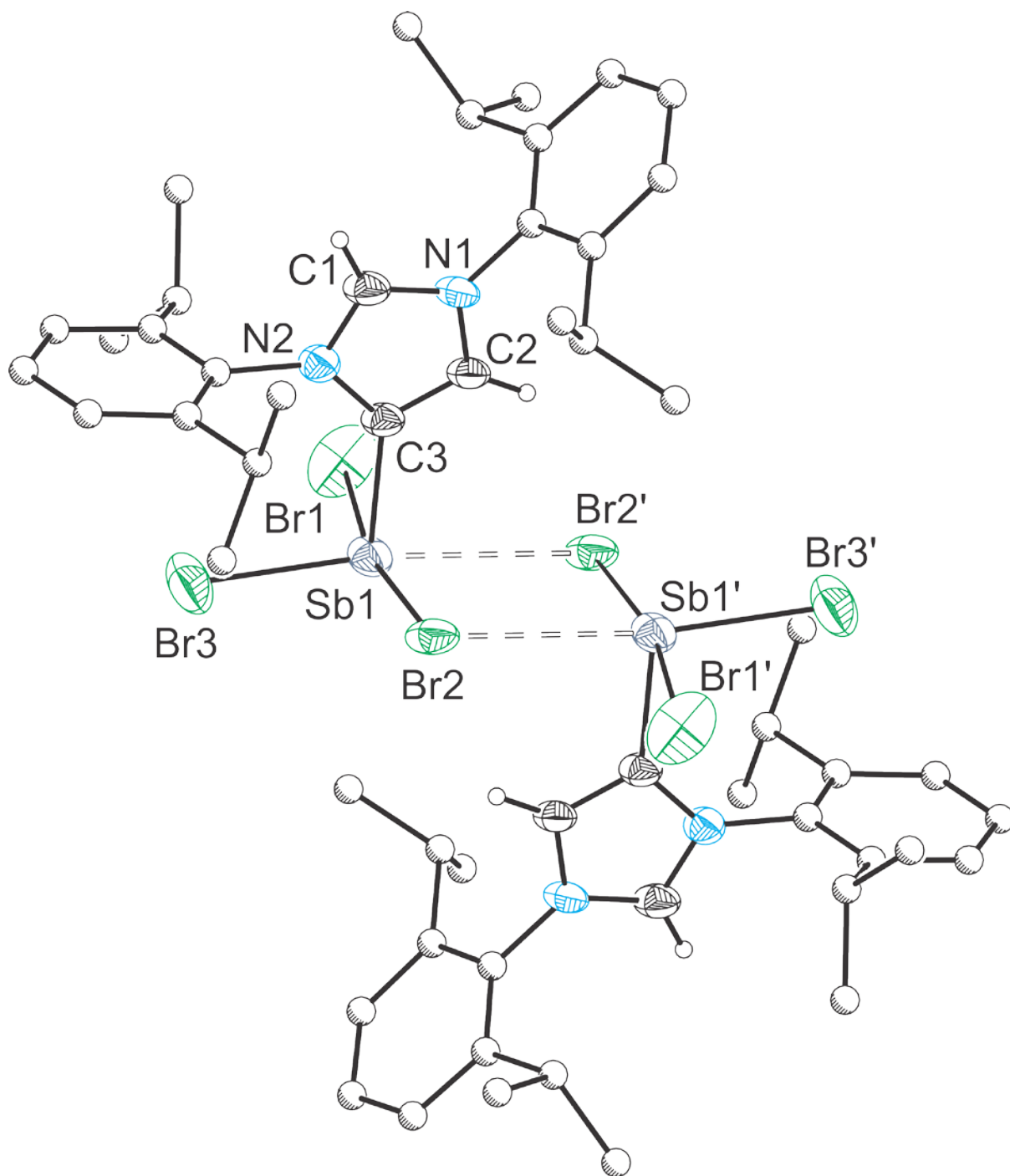


Figure 6. Molecular structure of the dimeric unit of **5** present in **5**·2THF. Anisotropic displacement ellipsoids pictured are set at 50% probability. Hydrogen atoms (with the exception of the imidazole protons) have been omitted for clarity. Atoms of the Dipp groups and hydrogen atoms are pictured as spheres of arbitrary radii. Symmetry operation \prime : $1-x$, $2-y$, $1-z$. Selected bond distances (Å) and angles (°): Sb1–Br1, 2.627(1); Sb1–Br2, 2.976(1); Sb1–Br3, 2.574(1); Sb1–C3, 2.182(3); Sb1···Br2', 3.129(1). Br1–Sb1–Br2, 168.76(2); Br1–Sb1–

Br3, 95.11(3); Br1–Sb1–C3, 89.43(9); Br1–Sb1–Br2', 88.46(2); Br2–Sb1–Br3, 93.71(2); Br2–Sb1–C3, 82.63(9); Br2–Sb1–Br2', 83.60(1); Br3–Sb1–C3, 96.72(9); Br3–Sb1–Br2', 172.59(2); C3–Sb1–Br2', 89.80(9).

5 crystallises as a dimer in the *P1* space group with a centre of inversion at the centre of the Sb1–Br2–Sb1'–Br2' rhombus. The central Sb₂Br₆ moiety is approximately planar with a root-mean-square deviation from planarity of 0.119 Å. This structure results from the formation of two bridging bromides (Br2 and Br2') which form due to the donation of electron density into the σ^* of the Sb1–Br3 bond. The central Sb1–Br2–Sb1'–Br2' moiety is approximately square with Sb1–Br2–Sb1' and Br2–Sb1–Br2' angles of 96.4(1)° and 83.60(1)°, respectively. There are also two THF molecules which are hydrogen bonded to the acidic imidazolium protons.

Unlike the dimeric structure observed for [(IPr)BiBr₃]₂ which formed a dimer due to donation of electron density into the Bi–C σ^* orbital, in **5**, the stronger electron donating ability of the imidazole backbone of the aIPr ligand, coupled with the reduced steric bulk from only one flanking N–Dipp group results in a shorter, stronger Sb–C bond. As a result, the energy of the σ^* is raised and correspondingly, the LUMO becomes that of the Sb–Br σ^* . This type of bonding motif has been seen in a handful of complexes bearing formally anionic carbon based ligands such as methyl and phenyl groups and have been isolated as both the *cis* and *trans* isomers.^[35,36] Only the *trans* isomer is observed upon crystallisation of **5** due to the large steric bulk of the aIPr ligand.

The geometry about the antimony atom can be described as a five-coordinate, square based pyramidal geometry which can be quantified by the τ_5 parameter which is 0.064. The lone pair of electrons on the antimony atom are stereochemically active and occupy a position

trans to the aIPr ligand. The Sb1–C3 bond length is shorter than those in **1** and **3** at 2.182(3) Å as expected, due to the greater nucleophilicity of the backbone imidazole carbon. Similarly, the terminal Sb–Br bond lengths were measured to be 2.574(1) and 2.627(1) Å which is approximately equal to or longer than previously discussed Sb–Br single bonds. The Sb–Br distances between the antimony centre and the two bridging bromide ligands are significantly longer at 2.976(1) and 3.129(1) Å, however, well within the range of the sum of van der Waals radii.

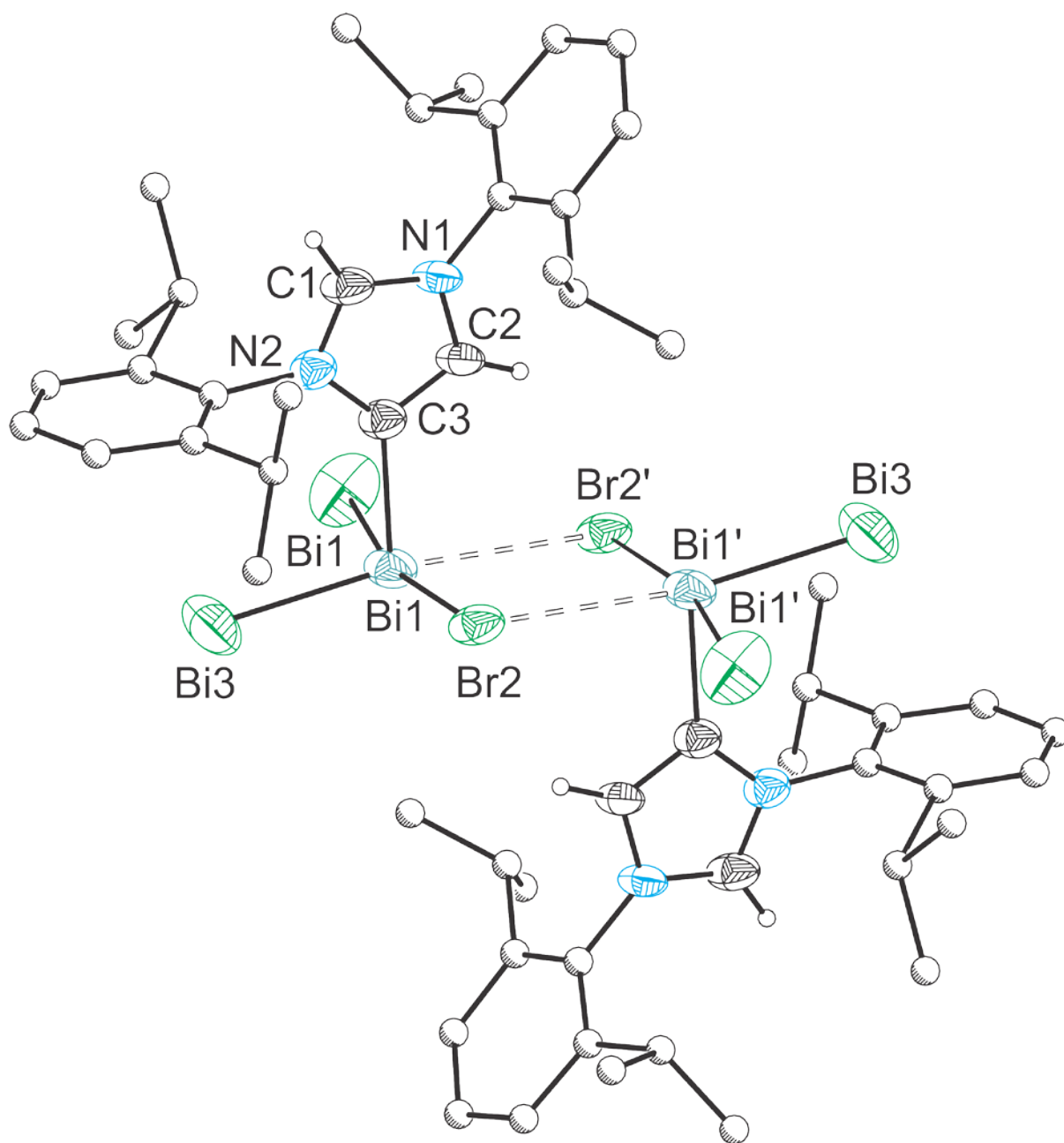


Figure 7. Molecular structure of the dimeric unit of **6** present in **6**·2THF. Anisotropic displacement ellipsoids pictured are set at 50% probability. Hydrogen atoms (with the exception of the imidazole protons) have been omitted for clarity. Atoms of the Dipp groups and hydrogen atoms are pictured as spheres of arbitrary radii. Symmetry operation i : $1-x, 2-y, 1-z$. Selected bond distances (Å) and angles (°): Bi1–Br1, 2.706(2); Bi1–Br2, 3.030(2); Bi1–Br3, 2.676(2); Bi1–C3, 2.277(6); Bi1···Br2', 3.072(1). Br1–Bi1–Br2, 167.92(3); Br1–Bi1–Br3, 96.09(5); Br1–Bi1–C3, 90.21(16); Br1–Bi1–Br2', 87.97(4); Br2–Bi1–Br3, 94.70(4); Br2–Bi1–C3, 83.07(16); Br2–Bi1–Br2', 82.03(3); Br3–Bi1–C3, 97.05(16); Br3–Bi1–Br2', 171.84(3); Br2'–Bi1–C3, 89.99(16).

Equivalent single crystals containing a dimeric structure of **6** were obtained and again, the two monomeric units are related by inversion symmetry in the *P1* space group. The Bi₂Br₆ moiety is approximately planar with a root-mean-square deviation from planarity of 0.116 Å. The central Bi1–Br2–Bi1'–Br2' is approximately square where the two internal angles Bi1–Br2–Bi1' and Br2–Bi1–Br2' are 97.97(3)° and 82.03(3)°, respectively. The Bi1–C3 bond length at 2.277(6) Å is shorter than those observed in **2** and **4** as expected. As in **5**, the terminal Bi–Br bonds are shorter than those to the bridging bromides at 2.676(1) and 2.706(2) Å which are slightly longer than that expected for a single Bi–Br bond. Those to the bridging bromides are significantly longer, as expected, at 3.030(2) and 3.072(1) Å and these distances are again, well within the sum of van der Waals radii for bismuth and bromine indicating reasonable interaction.

6 is also readily soluble in dichloromethane, and single crystals containing a tetrameric structure (a dimer of dimers) was obtained by diffusion of hexane into a dichloromethane solution and analysed by single crystal X-ray diffraction (Figure 8).

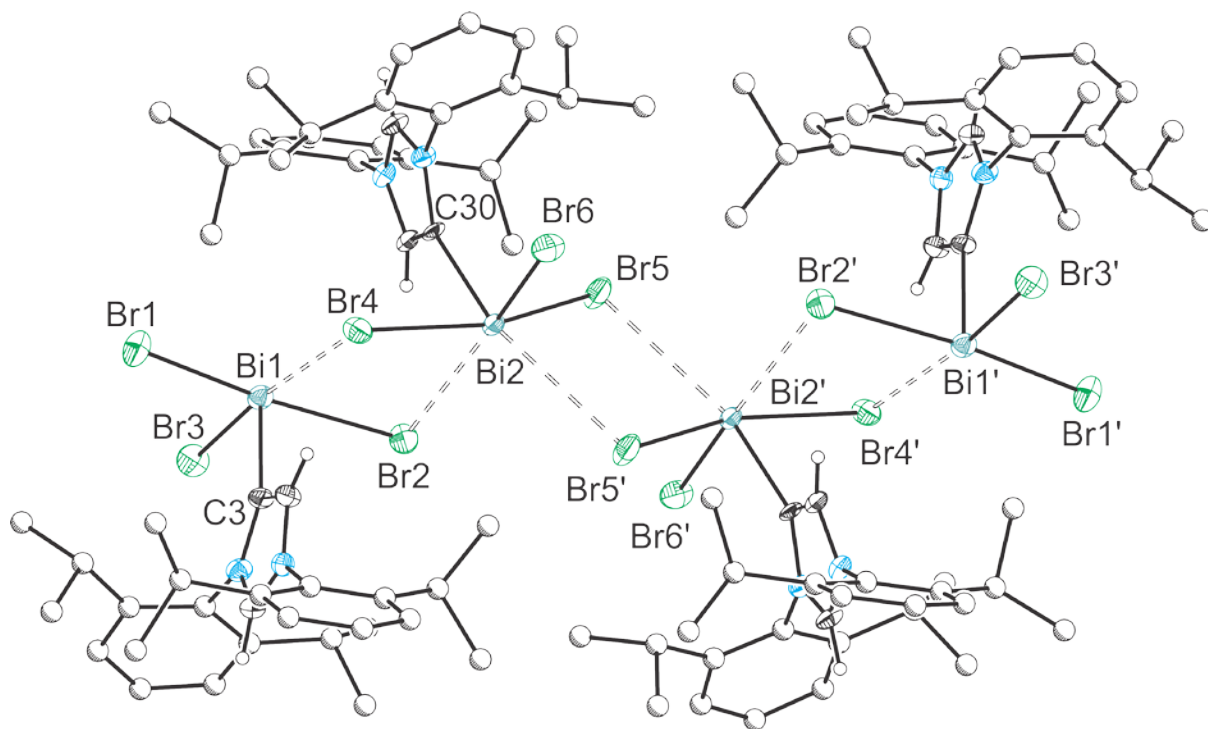


Figure 8. Molecular structure of the tetrameric unit of **6** present in **6**·0.5CH₂Cl₂. Anisotropic displacement ellipsoids pictured are set at 50% probability. Hydrogen atoms (with the exception of the imidazole protons) have been omitted for clarity. Atoms of the Dipp groups and hydrogen atoms are pictured as spheres of arbitrary radii. Symmetry operation \prime : $-x, -y, -z$. Selected bond distances (Å) and angles (°): Bi1–Br1, 2.770(1); Bi1–Br2, 2.931(1); Bi1–Br3, 2.690(1); Bi1–C3, 2.294(6); Bi1···Br4, 3.064(1); Bi2···Br2, 3.121(1); Bi2–Br4, 2.960(1); Bi2–Br5, 2.773(1); Bi2–Br6, 2.657(1); Bi2–C30, 2.310(5); Bi2···Br5', 3.399(1). Br1–Bi1–Br2, 171.20(2); Br1–Bi1–Br3, 97.00(3); Br1–Bi1–C3, 89.37(16); Br1–Bi1–Br4, 91.21(2); Br2–Bi1–Br3, 91.80(2); Br2–Bi1–C3, 89.66(16); Br2–Bi1–Br4, 80.00(2); Br3–Bi1–C3, 96.45(16); Br3–Bi1–Br4, 171.73(2); Br4–Bi1–C3, 84.65(16); Br4–Bi2–Br5, 163.90(2); Br4–Bi2–Br6, 86.00(2); Br4–Bi2–C30, 82.79(14); Br4–Bi2–Br2, 78.62(2); Br4–Bi2–Br5', 120.26(2); Br5–Bi2–Br6, 98.95(3); Br5–Bi2–C30, 81.34(14); Br5–Bi2–Br2, 98.71(2); Br5–Bi2–Br5', 75.39(2); Br6–Bi2–C30, 98.30(15); Br6–Bi2–Br2, 161.34(2); Br6–Bi2–Br5', 88.52(2); Br2–Bi2–C30, 90.26(15); Br5'–Bi2–C30, 156.51(14); Bi1–Br2–Bi2, 96.97(2); Bi1–Br4–Bi2, 97.60(2); Bi2–Br5–Bi2', 104.61(2).

The Bi₂Br₆ moiety of one dimer has been significantly distorted on formation of the tetramer as indicated by the root-mean-square deviation from planarity of 0.389 Å. Bi1 retains a square based pyramidal structure with τ_5 value of 0.009. Tetramerisation occurs by a similar means as that observed in [(IPr)BiBr₃]₂ whereby the formation of a second bridged bromide ligand to Bi2 is a result of donation of electron density, approximately into the σ^* of the Bi–C bond. However, there is significant structural distortion due to the presence of the stereochemically active lone pair which occupies a similar area in space as the Bi–C σ^* . The reduced hybridisation of s and p orbitals on bismuth results in the lone pair having significant s character, which allows for the distortion as the lone pair has little directionality. The Bi2–Br5' distance is significantly longer than other Bi–Br bonds at 3.399(1) Å, however, remains shorter than the sum of van der Waals radii (3.70 Å). Otherwise, all other bond metric data do not change by any appreciable degree.

Finally, computational studies also reveal that dimerisation of **5** and **6** is thermodynamically favourable by 40 and 45 kJ·mol^{–1}, respectively, and that these are also thermodynamically lower in energy than **1**·THF and the dimer of **2** by 11 and 16 kJ·mol^{–1}, respectively.

2.4. Bromide abstraction from **5** and **6**

With the aim of synthesising three-coordinate cationic group 15 dibromide species bearing an abnormally bonded IPr ligand (as opposed to with normal IPr ligands), we sought to react **5** and **6** with Na[B(3,5-{CF₃})₂C₆H₃)₄] (Na[BAr^F₄]) in order to abstract a bromide ligand by the favourable precipitation of NaBr. Accordingly, addition of one equivalent of the sodium salt with either **5** or **6** in dichloromethane results in immediate precipitation of NaBr (as determined by the absence of a resonance in the ²³Na NMR spectrum) and the formation of the cationic species [(aIPr)SbBr₂]⁺ (**7**) and [(aIPr)BiBr₂]⁺ (**8**).

Evidence for bromide abstraction and the formation of a cationic complex comes from the observable shifts in the resonances in the ^1H and $^{13}\text{C}\{^1\text{H}\}$ NMR spectra in CD_2Cl_2 coupled with the appearance of resonances attributable with the $[\text{BAr}^{\text{F}}_4]^-$ anion. All of the resonances in the ^1H NMR spectra of **7** and **8** undergo an upfield shift on bromide ion abstraction. This was observed for the imidazolium protons bonded to C2, which shift to 8.52 and 8.49 ppm for **7** and **8**, respectively (cf. 9.37 and 9.36 ppm for **5** and **6**). The same is also true for the resonances attributed to the alkenic C5-bonded proton (8.08 and 8.23 ppm for **7** and **8**, relative to 8.37 and 8.46 ppm for **5** and **6**, respectively) and the methine resonances (2.43/2.35 and 2.51/2.36 for **7** and **8**, relative to 3.06/2.64 and 3.00/2.57 ppm for **5** and **6**, respectively). The ^{13}C NMR resonance for the metal bonded carbanionic position also shifts to lower chemical shifts on abstraction of the bromide ion from 148.4 to 141.2 ppm on formation of **7**, and from 191.8 to 181.8 on formation of **8**.

Similarly conclusive evidence for the formation of the cationic species, **7** and **8**, comes from analysis of the samples by ESI-MS in dichloromethane. Analysis of $[\text{7}][\text{BAr}^{\text{F}}_4]$ by ESI-MS reveals a mass envelope at 669.8062 which can be ascribed to the molecular ion $[(\text{aIPr})\text{SbBr}_2]^+$ (Calcd 669.0266). Similarly, analysis of $[\text{8}][\text{BAr}^{\text{F}}_4]$ by ESI-MS reveals a mass envelope at 757.1990 which can be ascribed to the molecular ion $[(\text{aIPr})\text{BiBr}_2]^+$ (Calcd 757.1025).

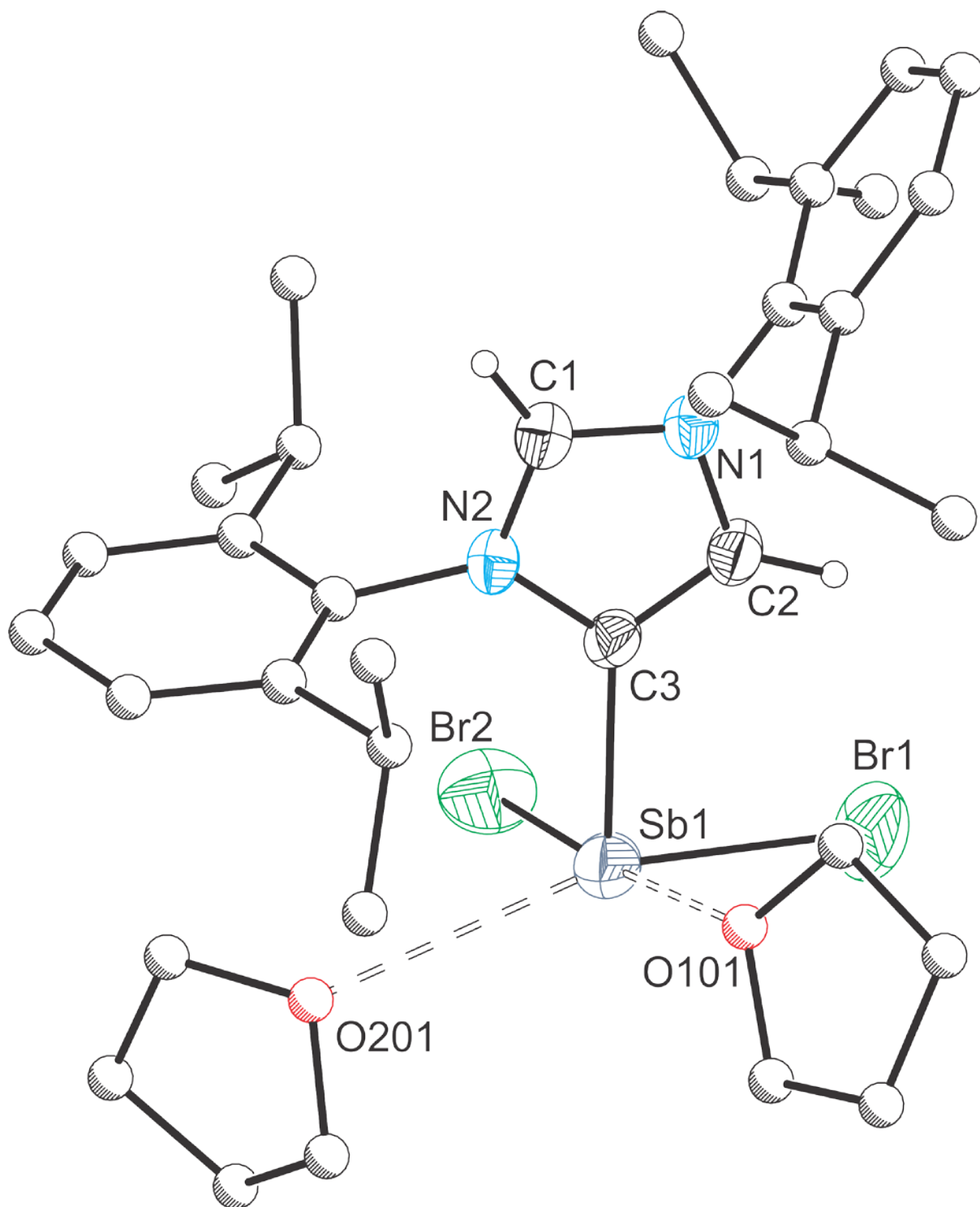


Figure 9. Structure of the cationic moiety present in $[7][\text{BARF}_4]\cdot 4\text{THF}$. Anisotropic displacement ellipsoids pictured are set at 50% probability. Hydrogen atoms (with the exception of the imidazole protons) and solvent of crystallisation that is not associated with the antimony(III) centre have been omitted for clarity. Atoms of the Dipp groups and hydrogen atoms are pictured as spheres of arbitrary radii. Sb1–Br1, 2.526(1); Sb1–Br2

2.5252(6); Sb1–C3, 2.184(3); Sb1···O101, 2.695(3); Sb1···O201, 2.936(4). Br1–Sb1–Br2, 93.44(3); Br1–Sb1–C3, 90.20(8); Br1–Sb1–O101, 84.56(9); Br1–Sb1–O201, 159.68(7); Br2–Sb1–C3, 95.70(8); Br2–Sb1–O101, 176.29(7); Br2–Sb1–O201, 81.64(8); C3–Sb1–O101, 81.21(11); C3–Sb1–O201, 109.84(11); O101–Sb1–O201, 101.30(11).

Both [7][BAr^F₄].4THF and [8][BAr^F₄].4.5THF were crystallised from THF with two molecules of THF coordinated to the group 15 element centre (Figures 9 and 10) along with additional molecules of THF in the lattice, several of which hydrogen bond to the protons of the imidazole rings. The coordination of the aIPr ligand and the two bromide ligands result in a trigonal pyramidal geometry as expected for both **7** and **8** and the coordination of two additional molecules of THF by donation of electron density into the two E–Br σ^* orbitals affords a distorted, square based pyramidal structure which can be quantified by the τ_5 value which is 0.277 for **7**·4THF. The longer bonds between the ligands and the bismuth centre in [8][BAr^F₄].4.5THF results in reduced steric clash which allows for greater square based pyramidal character as determined by the τ_5 value which is 0.148.

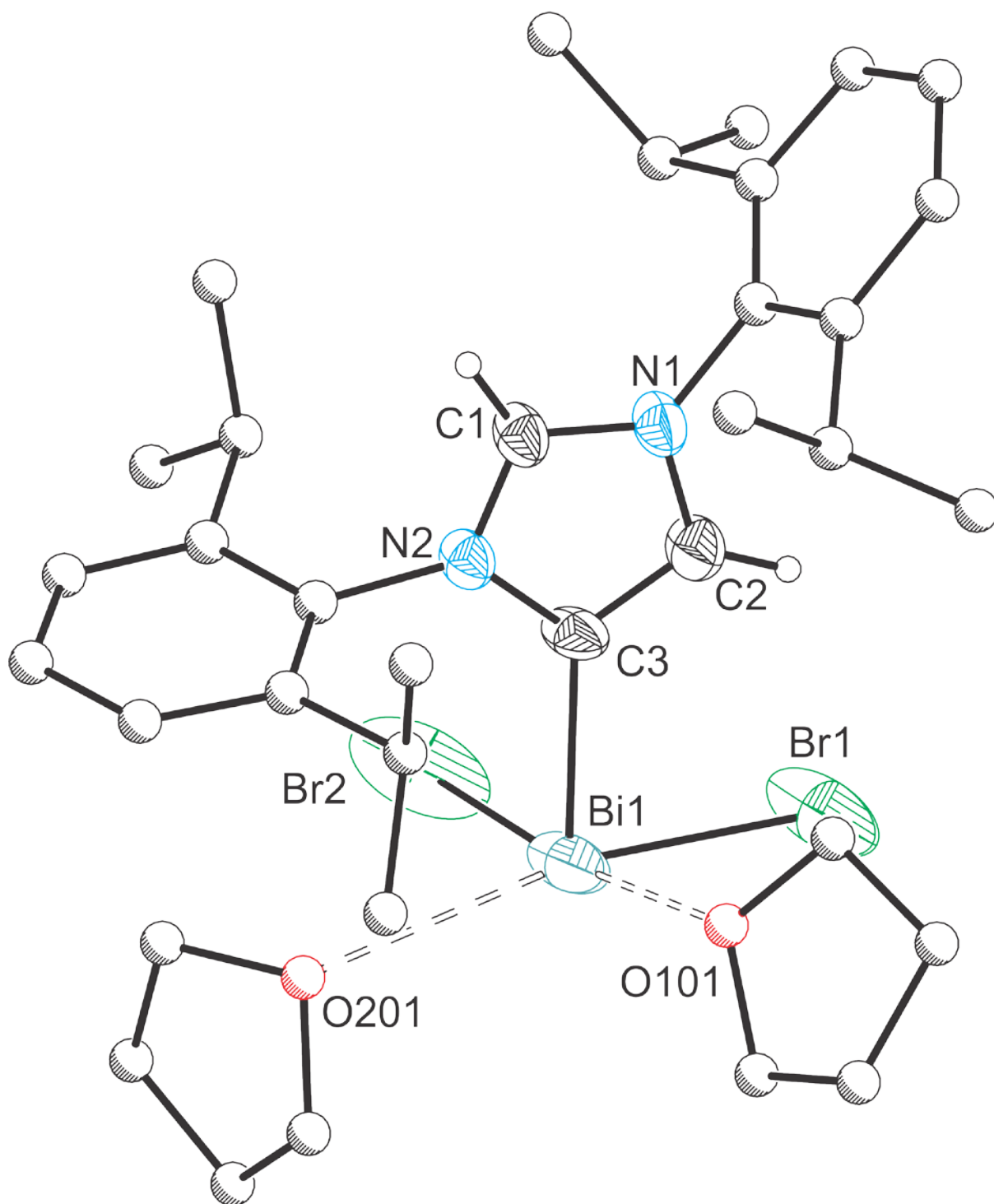


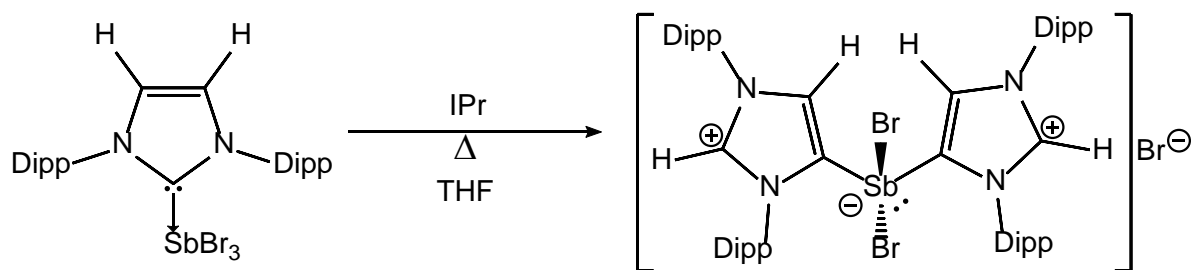
Figure 10. Structure of the cationic moiety present in $[8][\text{BAR}^{\text{F}}_4]\cdot 4.5\text{THF}$. Anisotropic displacement ellipsoids pictured are set at 50% probability. Hydrogen atoms (with the exception of the imidazole protons) and solvent of crystallisation that is not associated with the bismuth(III) centre have been omitted for clarity. Atoms of the Dipp groups and hydrogen atoms are pictured as spheres of arbitrary radii. Bi1–Br1, 2.653(1); Bi1–Br2 2.635(1); Bi1–

C3, 2.291(4); Bi1...O101, 2.673(5); Bi1...O201, 2.755(4). Br1–Bi1–Br2, 92.82(4); Br1–Bi1–C3, 89.47(11); Br1–Bi1–O101, 85.43(12); Br1–Bi1–O201, 164.34(9); Br2–Bi1–C3, 91.17(12); Br2–Bi1–O101, 173.19(10); Br2–Bi1–O201, 82.99(10); C3–Bi1–O101, 82.24(16); C3–Bi1–O201, 105.64(14); O101–Bi1–O201, 100.39(15).

The Sb1–C3 bond length in **7** was measured to be 2.184(3) Å which is significantly shorter than previously discussed Sb–C bond lengths due to the greater nucleophilicity of the backbone imidazole carbon coupled with the increase in electrophilicity of the antimony centre upon bromide abstraction. Likewise, the Bi1–C3 bond length at 2.291(4) Å is notably shorter than previously discussed Bi–C bond lengths for the same motive. Analogous arguments also explain the short Sb–Br bond lengths (2.525(1) and 2.526(1) Å) and Bi–Br bond lengths (2.635(2) and 2.653(1) Å) in **7** and **8**, respectively.

2.5. Isomerisation of two equivalents of IPr with EBr₃ (E = Sb, Bi)

The addition of a second equivalent of IPr to (IPr)SbBr₃ (or simply the addition of two equivalents of IPr to SbBr₃) followed by heating in THF results in the isomerisation of both equivalents of IPr and the resulting complex bears two abnormally bonded IPr ligands (Scheme 2).



Scheme 2. Reaction scheme for synthesis of [9]Br by heating a THF solution of two equivalents of IPr with SbBr₃.

During the reaction, colourless crystals of the product form in the reaction flask, the insolubility of which is a result of the ionic nature of the product which has liberated a bromide ion in place of the second aIPr ligand affording [(aIPr)₂SbBr₂]Br (**9**Br). The molecular structure of **9** was determined by single crystal X-ray diffraction and reveals a four-coordinate antimony centre coordinated by two aIPr ligands and two bromide ligands (Figure 11).

Reaction of **9**Br with either AlBr₃ or Na[BAr^F₄] in CH₂Cl₂ allows for isolation of **9** as the [AlBr₄][−] or [BAr^F₄][−] salts, respectively. The formation of [(aIPr)₂SbBr₂]⁺ was further evidenced by the presence of a mass envelope at 1057.4980 (Calcd 1057.3142) upon analysis of a sample of **9**[BAr^F₄] by ESI-MS in CH₂Cl₂.

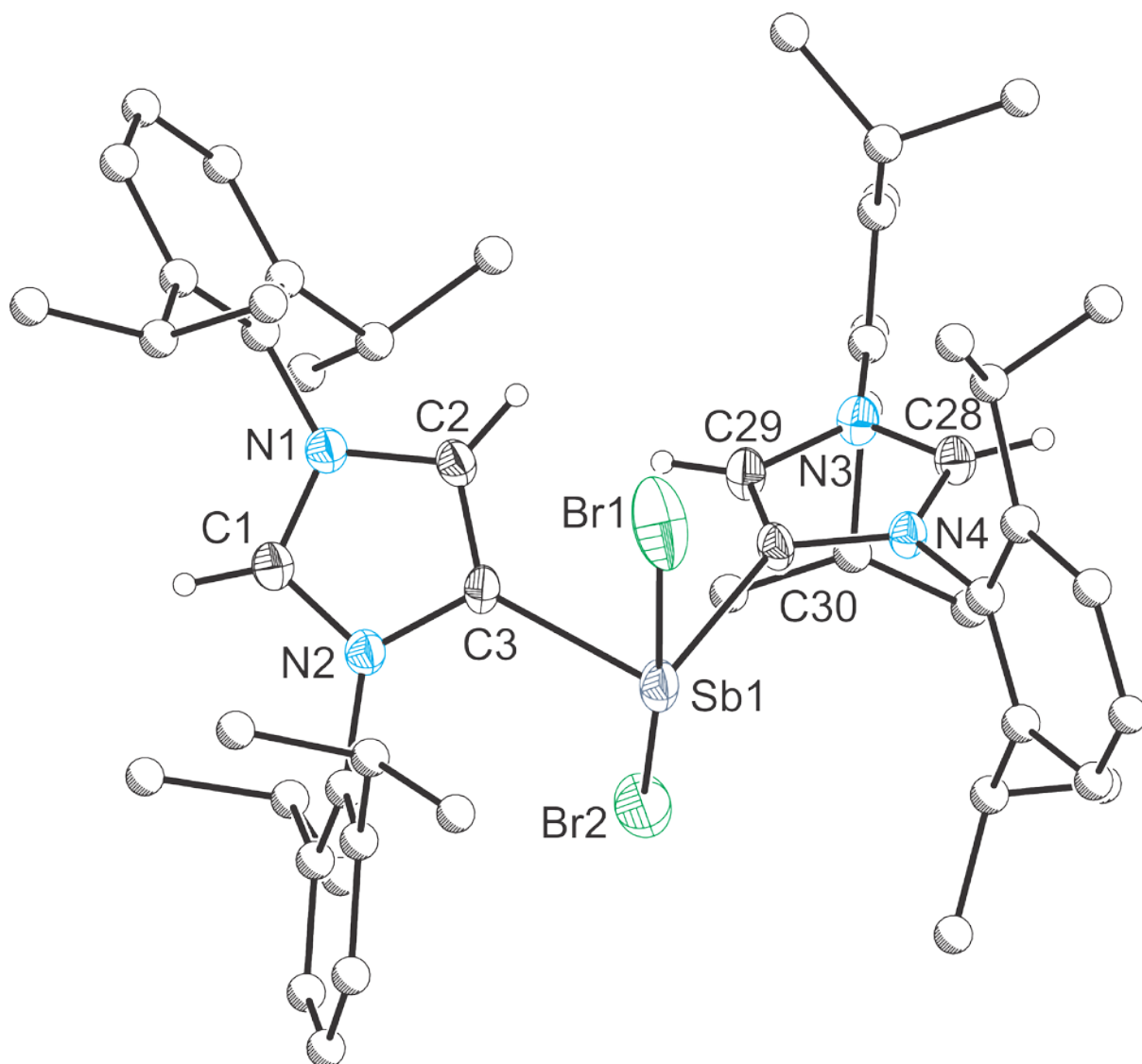


Figure 11. Molecular structure of the cationic moiety present in **[9][Br]**·0.5THF. Anisotropic displacement ellipsoids pictured are set at 50% probability. Hydrogen atoms (with the exception of the imidazole protons) and THF molecule have been omitted for clarity. Atoms of the Dipp groups, the THF molecule, and hydrogen atoms are pictured as spheres of arbitrary radii. Selected bond distances (Å) and angles (°): Sb1–Br1, 2.717(1); Sb1–Br2, 2.742(1); Sb1–C3, 2.163(2); Sb1–C30, 2.158(2). Br1–Sb1–Br2, 168.201(15); Br1–Sb1–C3, 84.27(7); Br1–Sb1–C30, 87.46(7); Br2–Sb1–C3, 86.96(7); Br2–Sb1–C30, 85.15(7); C3–Sb1–C30, 93.16(9).

Equivalent reactions with BiBr₃ do not give rise to isomerisation of the second equivalent of IPr. Extended heating at temperatures up to 100 °C in *d*₈-THF reveal the presence of only (aIPr)BiBr₃ (**6**) and free IPr. It may be that the acidity of the backbone proton of the coordinated IPr ligand is not sufficiently great for it to be abstracted by free IPr. An alternative mechanism relies on the autoionisation of IPr upon heating, generating small quantities of both [IPrH]⁺ and [aIPr][−] which may give rise to free aIPr and then proceed to react with other electrophiles in solution such as EBr₃. It may then be the case that there is no favourable energy gain on forming an additional aIPr–Bi bond due to the inherent weakness of Bi–C bonds, hence any free, uncoordinated aIPr in solution would favourably isomerise to afford IPr.

Computational studies reveal that isomerisation of a second equivalent of IPr to afford cation **9** is 59 kJ·mol^{−1} more favourable than the combination of **5** with an equivalent of free IPr. Formation of the product is strongly driven by the formation of an ionic salt which crystallises from the reaction solution as indicated by the interaction with the bromide ion which contributes an energy gain of 290 kJ·mol^{−1}. Likewise, the postulated formation of [(aIPr)₂BiBr₂]Br may be possible due to the ionic contribution which provides an energy gain of 287 kJ·mol^{−1}, however, this results in an overall thermodynamic energy gain of only 3 kJ·mol^{−1} relative to the precursors **6** and free IPr. This very small energy gain may easily be compensated for by the solvation of **6** which further disfavours the isomerisation of a second equivalent of IPr, hence no reaction is observed.

All salts of **9** may be crystallised by slow diffusion of hexane into THF or dichloromethane solutions and the bond metric data observed for **9** in all samples are similar, consequently only that of [9]Br will be discussed. Analysis of the molecular structure of **9** reveals a four-

coordinate antimony centre in a disphenoidal geometry with a τ_4' parameter of 0.380. The two aIPr ligands occupy an equatorial position forming two single Sb–C bonds (2.158(2) and 2.163(2) Å, cf. 2.165(3) Å for the only other structurally characterised aIPr complex of antimony, [(IPr)(aIPr)SbF₂]⁺),^[37] whilst the two bromide ligands occupy the axial positions and form part of a three-centre, four-electron bonding motif with the central antimony atom. As expected, the Sb–Br bond lengths are quite long at 2.717(1) and 2.742(1) Å due to the reduced bonding character between the antimony and the bromide ligands. The stereochemically active lone pair of electrons residing on the antimony centre occupies an equatorial position.

Finally, with the aim of investigating the possibility of the abstraction of a bromide ion from the cationic species, addition of two equivalents of Na[BAr^F₄] to **[9]**Br in dichloromethane resulted in the immediate precipitation of two equivalents of NaBr (as determined by the absence of a resonance in the ²³Na NMR spectrum when monitored in CD₂Cl₂). The resulting dicationic species, [(aIPr)₂SbBr]²⁺ (**10**), was isolated as a colourless, amorphous solid in 76% yield by removal of the solvent *in vacuo* after filtration from the NaBr. Analysis of **[10]**[BAr^F₄] by ESI-MS in CH₂Cl₂ reveals a mass envelope at 489.2816 (Calcd 489.1976) which can be ascribed to the dication, **10**, and exhibits an isotopic distribution whereby the peaks are separated by half a mass unit as a result of the dicationic charge. The ¹H NMR spectrum reveals a shift in the chemical shift of all resonances and the presence of the two imidazole proton resonances as two coupled doublets at 8.62 and 7.73 ppm. Consistent with that observed for other species bearing two aIPr ligands, restricted rotation about the N–Dipp bonds results in the doubling of a number of resonances in the ¹H and ¹³C{¹H} NMR spectra. Finally, the protonated C2 carbon, antimony bound carbon and the protonated alkenic imidazole carbon were found in the ¹³C{¹H} NMR spectrum at 140.9, 135.7 and 135.4 ppm.

Slow diffusion of hexane into CH₂Cl₂ or THF solutions results in the formation of a colourless oil which on standing for over two months gave rise to small colourless crystals suitable for single crystal X-ray diffraction. Analysis of the data reveals evidence for the dication, **10**, however this is accompanied with a second, disordered equivalent of **10** (as evidenced by the number of [BAr^F₄][−] anions in the unit cell) which lies on an inversion centre and cannot be accurately modelled.

Computational studies support the formation of the dication **10** as the Sb–Br bond dissociation energy in cation **9** was calculated to be 620 kJ·mol^{−1} and this is more than compensated for upon addition of Na[BAr^F₄] in a non-coordinating solvent by the precipitation of NaBr which has a lattice energy of 753 kJ·mol^{−1}.^[38]

3. Conclusions

We have shown that in contrast to their lighter homologue, (IPr)PBr₃, the 1:1 adducts of IPr with SbBr₃ and BiBr₃, (IPr)EBr₃ (E = Sb (**1**), Bi (**2**)), readily isomerise on thermal treatment to afford the abnormally-bonded (or mesoionic) complexes (aIPr)EBr₃ (E = Sb (**5**), Bi (**6**)). Bromide ion abstraction from all four compounds is possible using Lewis acids to afford the cationic compounds [(IPr)EBr₂]⁺ (E = Sb (**3**), Bi (**4**)) and [(aIPr)EBr₂]⁺ (E = Sb (**7**), Bi, (**8**)). Compound **7** readily reacts with a further equivalent of IPr to afford the cationic compound, [(aIPr)₂SbBr₂]⁺ (**9**), which features two abnormally bonded NHC ligands. This family of compounds are interesting precursors to low-valent, low-coordinate compounds of the heavier group 15 elements, and we are currently exploring their behaviour as precursors to such compounds.

4. Experimental details

4.1. General synthetic methods.

All reactions and product manipulations were carried out under an inert atmosphere of argon or dinitrogen using standard Schlenk-line or glovebox techniques (MBraun UNILab or MBraun LABmaster 130 glovebox maintained at <0.1 ppm H₂O and <0.1 ppm O₂). Diethyl ether (Et₂O; puriss. p.a., ACS reagent grade, ≥99.8%, Sigma-Aldrich) and tetrahydrofuran (THF; HPLC grade, ≥99.9%, Sigma-Aldrich) were distilled from a sodium or potassium/benzophenone mixture respectively. Dichloromethane (HPLC grade, ≥99.8%, Sigma-Aldrich) and hexane (HPLC grade, >97%, Sigma-Aldrich) were purified using an MBraun SPS-800 solvent system. CD₂Cl₂ (99.9%, Fluorochem) and *d*₈-THF (99.5%, Fluorochem) were dried over CaH₂, vacuum distilled and degassed before use. All dry solvents were stored under argon in gas-tight ampoules over activated 3 Å molecular sieves.

IPr was synthesised by a modification of literature procedures.^[39,40] To a suspension of [IPrH]Cl in Et₂O was added one equivalent of ^{*n*}BuLi (2.5 M in hexanes) slowly with stirring at ambient temperature and allowed to stir overnight. The solution was then filtered and stored at –80 °C to afford IPr as a crystalline material which was isolated by filtration and dried thoroughly under vacuum. Na[B(3,5-{CF₃})₂C₆H₃)₄] (Na[BAr^F₄]) was prepared according to a literature procedure.^[41] Additionally, Na[BAr^F₄] was recrystallised from a mixture of CH₂Cl₂ and Et₂O at –35 °C. BiBr₃ was prepared by refluxing bismuth chunks in bromine for five hours. Excess bromine was removed *in vacuo* and the BiBr₃ was redissolved in Et₂O, filtered and removal of the Et₂O under a dynamic vacuum afforded pure yellow crystalline BiBr₃. SbBr₃ was prepared by refluxing bromine with an excess of antimony shot in carbon tetrachloride until no bromine colour remained. After filtration of the warm reaction mixture, pale yellow crystals of the product forms on cooling which were then

isolated by filtration and dried carefully under vacuum. AlBr₃ (98%, Alfa Aesar) was used as received.

4.2. Compound syntheses

Synthesis of (IPr)SbBr₃ (1). To a suspension of IPr (536 mg, 1.383 mmol) in diethyl ether (15 mL) was added a solution of SbBr₃ (500 mg, 1.383 mmol) in diethyl ether (5 mL) while stirring at ambient temperature to afford a pale yellow solution and pale yellow precipitate. The mixture was stirred for one hour before the solution was filtered from the precipitate and the pale yellow solid dried thoroughly under vacuum (838 mg, 81% yield). Pale yellow crystals of (IPr)SbBr₃·2THF suitable for single crystal X-ray diffraction were grown from a saturated THF solution at –25 °C. Anal. Calcd for C₂₇H₃₆Br₃N₂Sb (750.06): C 43.24%, H 4.84%, N 3.74%. Found: C 42.80%, H 4.81%, N 3.70%. ¹H NMR (500.30 MHz, d₈-THF): δ (ppm) 7.92 (s, 2H; N(CH)₂N); 7.56 (t, ³J_{H-H} = 8 Hz, 2H; *para*-Dipp); 7.39 (d, ³J_{H-H} = 8 Hz, 4H; *meta*-Dipp); 3.21 (sept, ³J_{H-H} = 7 Hz, 4H; C₆H₃{CH(CH₃)₂})₂); 1.45 (d, ³J_{H-H} = 7 Hz, 12H; C₆H₃{CH(CH₃)₂})₂); 1.12 (d, ³J_{H-H} = 7 Hz, 12H; C₆H₃{CH(CH₃)₂})₂). ¹³C{¹H} NMR (125.80 MHz, d₈-THF): δ (ppm) 156.2 (CN₂); 148.0 (*ortho*-Dipp); 133.7 (*ipso*-Dipp); 132.7 (*para*-Dipp); 128.5 (N(CH)₂N); 125.4 (*meta*-Dipp); 30.1 (C₆H₃{CH(CH₃)₂})₂); 26.8, 24.0 (C₆H₃{CH(CH₃)₂})₂).

Synthesis of (IPr)BiBr₃ (2). To a suspension of IPr (754 mg, 1.943 mmol) in diethyl ether (30 mL) was added a solution of BiBr₃ (872 mg, 1.943 mmol) in diethyl ether (10 mL) while stirring at ambient temperature to afford a yellow solution and bright yellow precipitate. The mixture was stirred for one hour before the solution was filtered from the precipitate and the yellow solid dried thoroughly under vacuum (1.460 g, 90% yield). Yellow crystals of (IPr)BiBr₃·0.5THF suitable for single crystal X-ray diffraction were grown by slow diffusion

of hexane into a THF solution. Anal. Calcd for $C_{27}H_{36}BiBr_3N_2$ (837.28): C 38.73%, H 4.33%, N 3.35%. Found: C 38.60%, H 4.62%, N 3.35%. 1H NMR (500.30 MHz, d_8 -THF): δ (ppm) 7.79 (s, 2H; $N(CH)_2N$); 7.50 (t, $^3J_{H-H} = 8$ Hz, 2H; *para*-Dipp); 7.34 (d, $^3J_{H-H} = 8$ Hz, 4H; *meta*-Dipp); 3.16 (sept, $^3J_{H-H} = 7$ Hz, 4H; $C_6H_3\{CH(CH_3)_2\}_2$); 1.46 (d, $^3J_{H-H} = 7$ Hz, 12H; $C_6H_3\{CH(CH_3)_2\}_2$); 1.11 (d, $^3J_{H-H} = 7$ Hz, 12H; $C_6H_3\{CH(CH_3)_2\}_2$). $^{13}C\{^1H\}$ NMR (125.80 MHz, d_8 -THF): δ (ppm) 194.9 (v br, CN_2); 147.7 (*ortho*-Dipp); 135.2 (*ipso*-Dipp); 132.0 (*para*-Dipp); 128.7 ($N(CH)_2N$); 125.2 (*meta*-Dipp); 30.0 ($C_6H_3\{CH(CH_3)_2\}_2$); 26.7, 24.3 ($C_6H_3\{CH(CH_3)_2\}_2$).

Synthesis of [(IPr)SbBr₂][AlBr₄] ([3][AlBr₄]). To a mixture of (IPr)SbBr₃ (138 mg, 0.184 mmol) and AlBr₃ (49 mg, 0.184 mmol) was added CH₂Cl₂ (5 mL) while stirring at ambient temperature to afford a colourless solution. The mixture was stirred for 30 minutes before the solution was filtered and layered with hexane to afford colourless crystals of [(IPr)SbBr₂][AlBr₄]·0.5CH₂Cl₂ suitable for single crystal X-ray diffraction (147 mg, 79% crystalline yield). Anal. Calcd for $C_{27}H_{36}AlBr_6N_2Sb$ (1016.75): C 31.90%, H 3.57%, N 2.76%. Found: C 33.52%, H 3.82%, N 2.86%. ESI-MS, positive ion mode (CH₂Cl₂, 60 °C, 4.5 kV): m/z 669.1093 (100%) [(IPr)SbBr₂]⁺ (Calcd 669.0266). 1H NMR (500.30 MHz, CD₂Cl₂): δ (ppm) 7.78 (s, 2H; $N(CH)_2N$); 7.71 (t, $^3J_{H-H} = 8$ Hz, 2H; *para*-Dipp); 7.46 (d, $^3J_{H-H} = 8$ Hz, 4H; *meta*-Dipp); 2.50 (sept, $^3J_{H-H} = 7$ Hz, 4H; $C_6H_3\{CH(CH_3)_2\}_2$); 1.39 (d, $^3J_{H-H} = 7$ Hz, 12H; $C_6H_3\{CH(CH_3)_2\}_2$); 1.23 (d, $^3J_{H-H} = 7$ Hz, 12H; $C_6H_3\{CH(CH_3)_2\}_2$). $^{13}C\{^1H\}$ NMR (125.80 MHz, CD₂Cl₂): δ (ppm) 150.3 (CN_2); 146.0 (*ortho*-Dipp); 133.9 (*para*-Dipp); 130.5 (*ipso*-Dipp); 129.1 ($N(CH)_2N$); 125.9 (*meta*-Dipp); 30.0 ($C_6H_3\{CH(CH_3)_2\}_2$); 26.3, 23.2 ($C_6H_3\{CH(CH_3)_2\}_2$). ^{27}Al NMR (104.27 MHz, CD₂Cl₂): δ (ppm) 80.9 (s).

Synthesis of [(IPr)BiBr₂][AlBr₄] ([4][AlBr₄]). To a mixture of (IPr)BiBr₃ (225 mg, 0.269 mmol) and AlBr₃ (72 mg, 0.269 mmol) was added CH₂Cl₂ (5 mL) while stirring at ambient temperature to afford a pale yellow solution and pale yellow precipitate. The mixture was stirred for 30 minutes before the volatiles were removed in vacuo and the yellow solid dried thoroughly under vacuum (261 mg, 88% yield). Pale yellow crystals of [(IPr)BiBr₂][AlBr₄]·0.5CH₂Cl₂ suitable for single crystal X-ray diffraction were grown by slow diffusion of hexane into a CH₂Cl₂ solution. ESI-MS, positive ion mode (CH₂Cl₂, 60 °C, 4.5 kV): *m/z* 757.1798 (100%) [(IPr)BiBr₂]⁺ (Calcd 757.1025). ¹H NMR (500.30 MHz, CD₂Cl₂): δ (ppm) 7.69 (s and t, ³J_{H-H} = 8 Hz, 4H; N(CH)₂N and *para*-Dipp); 7.46 (d, ³J_{H-H} = 8 Hz, 4H; *meta*-Dipp); 2.55 (sept, ³J_{H-H} = 7 Hz, 4H; C₆H₃{CH(CH₃)₂})₂); 1.41 (d, ³J_{H-H} = 7 Hz, 12H; C₆H₃{CH(CH₃)₂})₂); 1.21 (d, ³J_{H-H} = 7 Hz, 12H; C₆H₃{CH(CH₃)₂})₂). ¹³C{¹H} NMR (125.80 MHz, CD₂Cl₂): δ (ppm) 191.3 (CN₂); 145.9 (*ortho*-Dipp); 133.6 (*para*-Dipp); 131.4 (*ipso*-Dipp); 129.1 (N(CH)₂N); 125.9 (*meta*-Dipp); 29.8 (C₆H₃{CH(CH₃)₂})₂); 26.3, 23.6 (C₆H₃{CH(CH₃)₂})₂). ²⁷Al NMR (104.27 MHz, CD₂Cl₂): δ (ppm) 81.1 (s).

Synthesis of (aIPr)SbBr₃ (5). To a solution of IPr (510 mg, 1.314 mmol) in an ampoule in THF (5 mL) was added a solution of SbBr₃ (475 mg, 1.314 mmol) in THF (5 mL) rapidly while stirring at ambient temperature to afford a colourless solution. The ampoule was then closed and the solution heated to 75 °C for three days before the solution was filtered. Hexane was allowed to diffuse slowly into this solution over the course of one week to afford large colourless crystals of (aIPr)SbBr₃·2THF suitable for single crystal X-ray diffraction. The supernatant was then decanted and the crystals dried thoroughly under vacuum (626 mg, 63% crystalline yield). Anal. Calcd for C₂₇H₃₆Br₃N₂Sb (750.06): C 43.24%, H 4.84%, N 3.74%. Found: C 43.65%, H 5.14%, N 3.36%. ¹H NMR (500.30 MHz, *d*₈-THF): δ (ppm) 9.37 (s, 1H; HCN₂); 8.37 (s, 1H; NCCHN); 7.63 (t, ³J_{H-H} = 8 Hz, 1H; *para*-Dipp); 7.59 (t, ³J_{H-H} =

8 Hz, 1H; *para*-Dipp); 7.47 (d, $^3J_{\text{H-H}} = 8$ Hz, 2H; *meta*-Dipp); 7.42 (d, $^3J_{\text{H-H}} = 8$ Hz, 2H; *meta*-Dipp); 3.06 (sept, $^3J_{\text{H-H}} = 7$ Hz, 2H; $\text{C}_6\text{H}_3\{\text{CH}(\text{CH}_3)_2\}_2$); 2.64 (sept, $^3J_{\text{H-H}} = 7$ Hz, 2H; $\text{C}_6\text{H}_3\{\text{CH}(\text{CH}_3)_2\}_2$); 1.44 (d, $^3J_{\text{H-H}} = 7$ Hz, 6H; $\text{C}_6\text{H}_3\{\text{CH}(\text{CH}_3)_2\}_2$); 1.30 (d, $^3J_{\text{H-H}} = 7$ Hz, 6H; $\text{C}_6\text{H}_3\{\text{CH}(\text{CH}_3)_2\}_2$); 1.23 (d, $^3J_{\text{H-H}} = 7$ Hz, 6H; $\text{C}_6\text{H}_3\{\text{CH}(\text{CH}_3)_2\}_2$); 1.11 (d, $^3J_{\text{H-H}} = 7$ Hz, 6H; $\text{C}_6\text{H}_3\{\text{CH}(\text{CH}_3)_2\}_2$). $^{13}\text{C}\{^1\text{H}\}$ NMR (125.80 MHz, d_8 -THF): δ (ppm) 148.4 (NCCHN); 147.3, 146.7 (*ortho*-Dipp); 140.1 (HCN_2); 135.6 (NCCHN); 132.9, 132.8 (*para*-Dipp); 132.3, 131.8 (*ipso*-Dipp); 125.6, 125.5 (*meta*-Dipp); 29.9, 29.8 ($\text{C}_6\text{H}_3\{\text{CH}(\text{CH}_3)_2\}_2$); 27.0, 24.8, 24.7, 23.6 ($\text{C}_6\text{H}_3\{\text{CH}(\text{CH}_3)_2\}_2$).

Synthesis of (aIPr)BiBr₃ (6). To a solution of IPr (258 mg, 0.665 mmol) in an ampoule in THF (5 mL) was added a solution of BiBr₃ (298 mg, 0.665 mmol) in THF (5 mL) rapidly while stirring at ambient temperature to afford a yellow solution. The ampoule was then closed and the solution heated to 75 °C overnight before the very pale yellow solution was layered with hexane to immediately afford colourless crystals. The supernatant was then decanted and the crystals dried thoroughly under vacuum (343 mg, 62% crystalline yield). Crystals of the dimer (aIPr)BiBr₃·2THF suitable for single crystal X-ray diffraction were grown by slow diffusion of hexane into a THF solution. Crystals of the tetramer (aIPr)BiBr₃·0.5CH₂Cl₂ were grown by slow diffusion of hexane into a CH₂Cl₂ solution. Anal. Calcd for C₂₇H₃₆BiBr₃N₂ (837.28): C 38.73%, H 4.33%, N 3.35%. Anal. Calcd for C₃₁H₄₄BiBr₃N₂O (909.39): C 40.94%, H 4.88%, N 3.08%. Found: C 40.08%, H 4.69%, N 3.06%. ^1H NMR (500.30 MHz, d_8 -THF): δ (ppm) 9.36 (d, $^4J_{\text{H-H}} = 2$ Hz, 1H; HCN_2); 8.46 (d, $^4J_{\text{H-H}} = 2$ Hz, 1H; NCCHN); 7.60 (t, $^3J_{\text{H-H}} = 8$ Hz, 1H; *para*-Dipp); 7.49 (t, $^3J_{\text{H-H}} = 8$ Hz, 1H; *para*-Dipp); 7.43 (d, $^3J_{\text{H-H}} = 8$ Hz, 2H; *meta*-Dipp); 7.32 (d, $^3J_{\text{H-H}} = 8$ Hz, 2H; *meta*-Dipp); 3.00 (sept, $^3J_{\text{H-H}} = 7$ Hz, 2H; $\text{C}_6\text{H}_3\{\text{CH}(\text{CH}_3)_2\}_2$); 2.57 (sept, $^3J_{\text{H-H}} = 7$ Hz, 2H; $\text{C}_6\text{H}_3\{\text{CH}(\text{CH}_3)_2\}_2$); 1.44 (d, $^3J_{\text{H-H}} = 7$ Hz, 6H; $\text{C}_6\text{H}_3\{\text{CH}(\text{CH}_3)_2\}_2$); 1.26 (d, $^3J_{\text{H-H}} = 7$ Hz, 6H; $\text{C}_6\text{H}_3\{\text{CH}(\text{CH}_3)_2\}_2$).

$\text{C}_6\text{H}_3\{\text{CH}(\text{CH}_3)_2\}_2$); 1.21 (d, $^3J_{\text{H-H}} = 7$ Hz, 6H; $\text{C}_6\text{H}_3\{\text{CH}(\text{CH}_3)_2\}_2$); 1.08 (d, $^3J_{\text{H-H}} = 7$ Hz, 6H; $\text{C}_6\text{H}_3\{\text{CH}(\text{CH}_3)_2\}_2$). $^{13}\text{C}\{^1\text{H}\}$ NMR (125.80 MHz, d_8 -THF): δ (ppm) 191.8 (v br, NCCHN); 147.5, 146.7 (*ortho*-Dipp); 141.8 (HCN_2); 141.0 (NCCHN); 134.0 (*ipso*-Dipp); 132.6, 132.0 (*para*-Dipp); 131.9 (*ipso*-Dipp); 125.5, 125.0 (*meta*-Dipp); 29.8 ($\times 2$) ($\text{C}_6\text{H}_3\{\text{CH}(\text{CH}_3)_2\}_2$); 26.7, 25.2, 24.5, 23.9 ($\text{C}_6\text{H}_3\{\text{CH}(\text{CH}_3)_2\}_2$). ^1H NMR (500.30 MHz, CD_2Cl_2): δ (ppm) 8.53 (d, $^4J_{\text{H-H}} = 2$ Hz, 1H; HCN_2); 8.20 (d, $^4J_{\text{H-H}} = 2$ Hz, 1H; NCCHN); 7.58 (t, $^3J_{\text{H-H}} = 8$ Hz, 2H; *para*-Dipp); 7.37 (d, $^3J_{\text{H-H}} = 8$ Hz, 2H; *meta*-Dipp); 7.35 (d, $^3J_{\text{H-H}} = 8$ Hz, 2H; *meta*-Dipp); 2.85 (sept, $^3J_{\text{H-H}} = 7$ Hz, 2H; $\text{C}_6\text{H}_3\{\text{CH}(\text{CH}_3)_2\}_2$); 2.46 (sept, $^3J_{\text{H-H}} = 7$ Hz, 2H; $\text{C}_6\text{H}_3\{\text{CH}(\text{CH}_3)_2\}_2$); 1.44 (d, $^3J_{\text{H-H}} = 7$ Hz, 6H; $\text{C}_6\text{H}_3\{\text{CH}(\text{CH}_3)_2\}_2$); 1.28 (d, $^3J_{\text{H-H}} = 7$ Hz, 6H; $\text{C}_6\text{H}_3\{\text{CH}(\text{CH}_3)_2\}_2$); 1.19 (d, $^3J_{\text{H-H}} = 7$ Hz, 6H; $\text{C}_6\text{H}_3\{\text{CH}(\text{CH}_3)_2\}_2$); 1.05 (d, $^3J_{\text{H-H}} = 7$ Hz, 6H; $\text{C}_6\text{H}_3\{\text{CH}(\text{CH}_3)_2\}_2$). $^{13}\text{C}\{^1\text{H}\}$ NMR (125.80 MHz, CD_2Cl_2): δ (ppm) 188.1 (br, NCCHN); 146.8, 145.8 (*ortho*-Dipp); 141.6 (HCN_2); 138.4 (NCCHN); 132.4 (*ipso*-Dipp); 132.3, 132.1 (*para*-Dipp); 130.2 (*ipso*-Dipp); 125.1, 124.8 (*meta*-Dipp); 29.4, 29.3 ($\text{C}_6\text{H}_3\{\text{CH}(\text{CH}_3)_2\}_2$); 26.7, 25.0, 24.4, 23.4 ($\text{C}_6\text{H}_3\{\text{CH}(\text{CH}_3)_2\}_2$).

Synthesis of [(aIPr)SbBr₂][BAr^F₄] ([7][BAr^F₄]). To a mixture of (aIPr)SbBr₃ (82 mg, 0.109 mmol) and Na[BAr^F₄] (97 mg, 0.109 mmol) was added CH_2Cl_2 (5 mL) rapidly while stirring at ambient temperature to afford a colourless solution and colourless precipitate. The solution was stirred for one hour then filtered and the volatiles removed in vacuo to afford a colourless solid. The solid was then dissolved in THF, filtered, then layered with hexane to afford colourless crystals of [(aIPr)SbBr₂(THF)₂][BAr^F₄] \cdot 2THF suitable for single crystal X-ray diffraction. (122 mg, 73% crystalline yield). Anal. Calcd for $\text{C}_{59}\text{H}_{48}\text{BBr}_2\text{F}_{24}\text{N}_2\text{Sb}$ (1533.37): C 46.21%, H 3.16%, N 1.83%. Anal. Calcd for $\text{C}_{67}\text{H}_{64}\text{BBr}_2\text{F}_{24}\text{N}_2\text{O}_2\text{Sb}$ (1677.58): C 47.97%, H 3.85%, N 1.67%. Found: C 47.88%, H 3.46%, N 1.92%. ESI-MS, positive ion mode (CH_2Cl_2 , 60 °C, 4.5 kV): m/z 669.0862 (100%) [(aIPr)SbBr₂]⁺ (Calcd 669.0266), 625.12914

(37%) [(aIPr)SbBr(OH)(OH₂)]⁺ (Calcd 625.1211), 607.1596 (88%) [(aIPr)SbBr(OH)]⁺ (Calcd 607.1106), 581.1702 (4%) [(aIPr)Sb(OH)₂(OH₂)₂]⁺ (Calcd 581.2183), 563.2008 (27%) [(aIPr)Sb(OH)₂(OH₂)]⁺ (Calcd 563.2077), 543.2307 (15%) [(aIPr)Sb(OH)₂]⁺ (Calcd 543.1966). ¹H NMR (500.30 MHz, CD₂Cl₂): δ (ppm) 8.52 (d, ⁴J_{H-H} = 2 Hz, 1H; HCN₂); 8.08 (d, ⁴J_{H-H} = 2 Hz, 1H; NCCHN); 7.72 (m, 9H; BC(CH)₂(CCF₃)₂CH and *para*-Dipp); 7.68 (t, ³J_{H-H} = 8 Hz, 1H; *para*-Dipp); 7.56 (s, 4H; BC(CH)₂(CCF₃)₂CH); 7.50 (d, ³J_{H-H} = 8 Hz, 2H; *meta*-Dipp); 7.45 (d, ³J_{H-H} = 8 Hz, 2H; *meta*-Dipp); 2.43 (sept, ³J_{H-H} = 7 Hz, 2H; C₆H₃{CH(CH₃)₂})₂); 2.35 (sept, ³J_{H-H} = 7 Hz, 2H; C₆H₃{CH(CH₃)₂})₂); 1.39 (d, ³J_{H-H} = 7 Hz, 6H; C₆H₃{CH(CH₃)₂})₂); 1.31 (d, ³J_{H-H} = 7 Hz, 6H; C₆H₃{CH(CH₃)₂})₂); 1.23 (d, ³J_{H-H} = 7 Hz, 6H; C₆H₃{CH(CH₃)₂})₂); 1.17 (d, ³J_{H-H} = 7 Hz, 6H; C₆H₃{CH(CH₃)₂})₂). ¹³C{¹H} NMR (125.80 MHz, CD₂Cl₂): δ (ppm) 162.2 (m, ¹J_{13C-11B} = 50 Hz, ¹J_{13C-10B} = 17 Hz; BC(CH)₂(CCF₃)₂CH); 145.5, 145.2 (*ortho*-Dipp); 141.3 (NCCHN); 139.5 (HCN₂); 135.2 (BC(CH)₂(CCF₃)₂CH and NCCHN); 134.6, 133.6 (*para*-Dipp); 129.3 (qq, ²J_{13C-19F} = 31 Hz, ⁴J_{13C-19F} = 2 Hz; BC(CH)₂(CCF₃)₂CH); 129.3, 129.2 (*ipso*-Dipp); 126.5, 125.8 (*meta*-Dipp); 125.1 (q, ¹J_{13C-19F} = 271 Hz; BC(CH)₂(CCF₃)₂CH); 117.9 (sept, ³J_{13C-19F} = 4 Hz; BC(CH)₂(CCF₃)₂CH); 30.0, 29.8 (C₆H₃{CH(CH₃)₂})₂); 26.4, 24.6, 24.1, 23.0 (C₆H₃{CH(CH₃)₂})₂). ¹¹B NMR (128.39 MHz, CD₂Cl₂): δ (ppm) -6.6 (s). ¹⁹F NMR (376.54 MHz, CD₂Cl₂): δ (ppm) -62.8 (s).

Synthesis of [(aIPr)BiBr₂][BAr^F₄] ([8][BAr^F₄]). To a mixture of (aIPr)BiBr₃ (40 mg, 0.048 mmol) and Na[BAr^F₄] (42 mg, 0.048 mmol) was added CH₂Cl₂ (5 mL) rapidly while stirring at ambient temperature to afford a pale yellow solution and colourless precipitate. The solution was stirred for one hour then filtered and the volatiles removed *in vacuo* to afford a colourless solid. The solid was then dissolved in THF, filtered, then layered with hexane to afford colourless crystals of [(aIPr)BiBr₂(THF)₂][BAr^F₄].2THF suitable for single crystal X-

ray diffraction. (55 mg, 71% crystalline yield). Anal. Calcd for $C_{59}H_{48}BBiBr_2F_{24}N_2$ (1620.59): C 43.73%, 2.99%, 1.73%. Anal. Calcd for $C_{67}H_{64}BBiBr_2F_{24}N_2O_2$ (1764.80): C 45.60%, H 3.66%, N 1.59%. Found: C 45.20%, H 3.18%, N 1.74%. ESI-MS, positive ion mode (CH_2Cl_2 , 60 °C, 4.5 kV): m/z 757.1990 (100%) $[(aIPr)BiBr_2]^+$ (Calcd 757.1025). 1H NMR (500.30 MHz, CD_2Cl_2): δ (ppm) 8.49 (d, $^4J_{H-H} = 2$ Hz, 1H; HCN_2); 8.23 (d, $^4J_{H-H} = 2$ Hz, 1H; $NCCHN$); 7.73 (m, 9H; $BC(CH)_2(CCF_3)_2CH$ and *para*-Dipp); 7.66 (t, $^3J_{H-H} = 8$ Hz, 1H; *para*-Dipp); 7.56 (s, 4H; $BC(CH)_2(CCF_3)_2CH$); 7.50 (d, $^3J_{H-H} = 8$ Hz, 2H; *meta*-Dipp); 7.44 (d, $^3J_{H-H} = 8$ Hz, 2H; *meta*-Dipp); 2.51 (sept, $^3J_{H-H} = 7$ Hz, 2H; $C_6H_3\{CH(CH_3)_2\}_2$); 2.36 (sept, $^3J_{H-H} = 7$ Hz, 2H; $C_6H_3\{CH(CH_3)_2\}_2$); 1.40 (d, $^3J_{H-H} = 7$ Hz, 6H; $C_6H_3\{CH(CH_3)_2\}_2$); 1.31 (d, $^3J_{H-H} = 7$ Hz, 6H; $C_6H_3\{CH(CH_3)_2\}_2$); 1.23 (d, $^3J_{H-H} = 7$ Hz, 6H; $C_6H_3\{CH(CH_3)_2\}_2$); 1.16 (d, $^3J_{H-H} = 7$ Hz, 6H; $C_6H_3\{CH(CH_3)_2\}_2$). $^{13}C\{^1H\}$ NMR (125.80 MHz, CD_2Cl_2): δ (ppm) 181.8 (v br, $NCCHN$); 162.2 (m, $^1J_{^{13}C-^{11}B} = 50$ Hz, $^1J_{^{13}C-^{10}B} = 17$ Hz; $BC(CH)_2(CCF_3)_2CH$); 145.5, 145.3 (*ortho*-Dipp); 141.2 ($NCCHN$); 140.5 (HCN_2); 135.2 ($BC(CH)_2(CCF_3)_2CH$); 134.3, 133.4 (*para*-Dipp); 130.1, 129.4 (*ipso*-Dipp); 129.3 (qq, $^2J_{^{13}C-^{19}F} = 31$ Hz, $^4J_{^{13}C-^{19}F} = 2$ Hz; $BC(CH)_2(CCF_3)_2CH$); 126.5, 125.7 (*meta*-Dipp); 125.1 (q, $^1J_{^{13}C-^{19}F} = 271$ Hz; $BC(CH)_2(CCF_3)_2CH$); 117.9 (sept, $^3J_{^{13}C-^{19}F} = 4$ Hz; $BC(CH)_2(CCF_3)_2CH$); 29.8, 29.7 ($C_6H_3\{CH(CH_3)_2\}_2$); 26.5, 24.6, 24.2, 23.2 ($C_6H_3\{CH(CH_3)_2\}_2$).

*Synthesis of $[(aIPr)_2SbBr_2]Br$ (**9**Br).* To a solution of IPr (555 mg, 1.430 mmol) in an ampoule in THF (5 mL) was added a solution of $SbBr_3$ (259 mg, 0.715 mmol) in THF (5 mL) rapidly while stirring at ambient temperature to afford a colourless solution. The ampoule was then closed and the solution heated to 80 °C overnight to afford large colourless crystals of **9**Br·0.5THF suitable for single crystal X-ray diffraction. The supernatant was then decanted and the crystals dried thoroughly under vacuum (785 mg, 96% crystalline yield). Anal. Calcd for $C_{54}H_{72}Br_3N_4Sb$ (1138.65): C 56.96%, H 6.37%, N 4.92%. Anal. Calcd for

C₅₈H₈₀Br₃N₄OSb (1210.75): C 57.54%, H 6.66%, N 4.63%. Found: C 57.70%, H 6.58%, N 4.71%. ¹H NMR (500.30 MHz, CD₂Cl₂): δ (ppm) 9.71 (s, 2H; HCN₂); 7.60 (s, 2H; NCCHN); 7.60 (t, ³J_{H-H} = 8 Hz, 4H; *para*-Dipp); 7.38 (d, ³J_{H-H} = 8 Hz, 4H; *meta*-Dipp); 7.36 (d, ³J_{H-H} = 8 Hz, 4H; *meta*-Dipp); 2.73 (sept, ³J_{H-H} = 7 Hz, 4H; C₆H₃{CH(CH₃)₂})₂); 2.46 (sept, ³J_{H-H} = 7 Hz, 4H; C₆H₃{CH(CH₃)₂})₂); 1.38 (d, ³J_{H-H} = 7 Hz, 12H; C₆H₃{CH(CH₃)₂})₂); 1.22 (d, ³J_{H-H} = 7 Hz, 12H; C₆H₃{CH(CH₃)₂})₂); 1.14 (d, ³J_{H-H} = 7 Hz, 24H; C₆H₃{CH(CH₃)₂})₂). ¹³C{¹H} NMR (125.80 MHz, CD₂Cl₂): δ (ppm) 146.2, 145.5 (*ortho*-Dipp); 143.4 (NCCHN); 139.2 (HCN₂); 133.8 (NCCHN); 132.7, 132.5 (*para*-Dipp); 130.9, 130.1 (*ipso*-Dipp); 125.3, 125.2 (*meta*-Dipp); 29.6, 29.4 (C₆H₃{CH(CH₃)₂})₂); 27.0, 24.5, 24.4, 22.8 (C₆H₃{CH(CH₃)₂})₂).

Synthesis of [(aIPr)₂SbBr₂][BAr^F₄] ([9][BAr^F₄]). To a mixture of [(aIPr)₂SbBr₂]Br (82 mg, 0.068 mmol) and Na[BAr^F₄] (60 mg, 0.068 mmol) was added CH₂Cl₂ (5 mL) while stirring at ambient temperature to afford a colourless solution and colourless precipitate. The solution was stirred for one hour then filtered and the volatiles removed in vacuo to afford a colourless solid. The solid was then dissolved in THF, filtered, then layered with hexane to afford colourless crystals of [(aIPr)₂SbBr₂][BAr^F₄].3THF suitable for single crystal X-ray diffraction. (93 mg, 72% crystalline yield). Anal. Calcd for C₈₆H₈₄BBBr₂F₂₄N₄Sb (1921.96): C 53.74%, H 4.41%, N 2.92%. Anal. Calcd for C₉₈H₁₀₈BBBr₂F₂₄N₄O₃Sb (2138.27): C 55.05%, H 5.09%, N 2.62%. Found: C 55.46%, H 5.04%, N 2.64%. ESI-MS, positive ion mode (CH₂Cl₂, 60 °C, 4.5 kV): *m/z* 1057.4980 (100%) [(aIPr)₂SbBr₂]⁺ (Calcd 1057.3142). ¹H NMR (500.30 MHz, CD₂Cl₂): δ (ppm) 8.94 (s, 2H; HCN₂); 7.74 (s, 8H; BC(CH)₂(CCF₃)₂CH); 7.65 (s, 2H; NCCHN); 7.63 (t, ³J_{H-H} = 8 Hz, 2H; *para*-Dipp); 7.60 (t, ³J_{H-H} = 8 Hz, 2H; *para*-Dipp); 7.56 (s, 4H; BC(CH)₂(CCF₃)₂CH); 7.41 (d, ³J_{H-H} = 8 Hz, 4H; *meta*-Dipp); 7.38 (d, ³J_{H-H} = 8 Hz, 4H; *meta*-Dipp); 2.75 (sept, ³J_{H-H} = 7 Hz, 4H; C₆H₃{CH(CH₃)₂})₂); 2.45 (sept, ³J_{H-H} = 7 Hz, 4H; C₆H₃{CH(CH₃)₂})₂); 1.41 (d, ³J_{H-H} = 7 Hz, 12H; C₆H₃{CH(CH₃)₂})₂); 1.20

(d, $^3J_{\text{H-H}} = 7$ Hz, 12H; $\text{C}_6\text{H}_3\{\text{CH}(\text{CH}_3)_2\}_2$); 1.16 (d, $^3J_{\text{H-H}} = 7$ Hz, 12H; $\text{C}_6\text{H}_3\{\text{CH}(\text{CH}_3)_2\}_2$); 1.11 (d, $^3J_{\text{H-H}} = 7$ Hz, 12H; $\text{C}_6\text{H}_3\{\text{CH}(\text{CH}_3)_2\}_2$). $^{13}\text{C}\{^1\text{H}\}$ NMR (125.80 MHz, CD_2Cl_2): δ (ppm) 162.2 (m, $^1J_{^{13}\text{C}-^{11}\text{B}} = 50$ Hz, $^1J_{^{13}\text{C}-^{10}\text{B}} = 17$ Hz; $\text{BC}(\text{CH})_2(\text{CCF}_3)_2\text{CH}$); 146.1, 145.5 (*ortho*-Dipp); 144.3 (NCCHN); 137.6 (HCN_2); 135.3 ($\text{BC}(\text{CH})_2(\text{CCF}_3)_2\text{CH}$); 133.9 (NCCHN); 133.1, 133.0 (*para*-Dipp); 130.7, 129.7 (*ipso*-Dipp); 129.3 (qq, $^2J_{^{13}\text{C}-^{19}\text{F}} = 31$ Hz, $^4J_{^{13}\text{C}-^{19}\text{F}} = 2$ Hz; $\text{BC}(\text{CH})_2(\text{CCF}_3)_2\text{CH}$); 125.6, 125.5 (*meta*-Dipp); 125.1 (q, $^1J_{^{13}\text{C}-^{19}\text{F}} = 271$ Hz; $\text{BC}(\text{CH})_2(\text{CCF}_3)_2\text{CH}$); 117.9 (sept, $^3J_{^{13}\text{C}-^{19}\text{F}} = 4$ Hz; $\text{BC}(\text{CH})_2(\text{CCF}_3)_2\text{CH}$); 29.7, 29.5 ($\text{C}_6\text{H}_3\{\text{CH}(\text{CH}_3)_2\}_2$); 27.0, 25.5, 25.4, 22.7 ($\text{C}_6\text{H}_3\{\text{CH}(\text{CH}_3)_2\}_2$). ^{11}B NMR (128.39 MHz, CD_2Cl_2): δ (ppm) -6.6 (s). ^{19}F NMR (376.54 MHz, CD_2Cl_2): δ (ppm) -62.8 (s).

Synthesis of [(aIPr)₂SbBr₂][AlBr₄] ([9][AlBr₄]). To a mixture of [(aIPr)₂SbBr₂]Br (90 mg, 0.079 mmol) and AlBr₃ (21 mg, 0.079 mmol) was added CH_2Cl_2 (5 mL) while stirring at ambient temperature to afford a colourless solution. The solution was stirred for one hour then filtered and layered with hexane to afford colourless crystals suitable for single crystal X-ray diffraction. (82 mg, 74% crystalline yield). Anal. Calcd for $\text{C}_{54}\text{H}_{72}\text{AlBr}_6\text{N}_4\text{Sb}$ (1405.34): C 46.15%, H 5.16%, N 3.99%. Found: C 45.87%, H 5.19%, N 3.99%. ^1H NMR (500.30 MHz, CD_2Cl_2): δ (ppm) 8.31 (d, $^4J_{\text{H-H}} = 2$ Hz, 2H; HCN_2); 7.68 (d, $^4J_{\text{H-H}} = 2$ Hz, 2H; NCCHN); 7.66 (t, $^3J_{\text{H-H}} = 8$ Hz, 2H; *para*-Dipp); 7.64 (t, $^3J_{\text{H-H}} = 8$ Hz, 2H; *para*-Dipp); 7.42 (d, $^3J_{\text{H-H}} = 8$ Hz, 8H; *meta*-Dipp); 2.75 (sept, $^3J_{\text{H-H}} = 7$ Hz, 4H; $\text{C}_6\text{H}_3\{\text{CH}(\text{CH}_3)_2\}_2$); 2.44 (sept, $^3J_{\text{H-H}} = 7$ Hz, 4H; $\text{C}_6\text{H}_3\{\text{CH}(\text{CH}_3)_2\}_2$); 1.41 (d, $^3J_{\text{H-H}} = 7$ Hz, 12H; $\text{C}_6\text{H}_3\{\text{CH}(\text{CH}_3)_2\}_2$); 1.21 (d, $^3J_{\text{H-H}} = 7$ Hz, 12H; $\text{C}_6\text{H}_3\{\text{CH}(\text{CH}_3)_2\}_2$); 1.18 (d, $^3J_{\text{H-H}} = 7$ Hz, 12H; $\text{C}_6\text{H}_3\{\text{CH}(\text{CH}_3)_2\}_2$); 1.11 (d, $^3J_{\text{H-H}} = 7$ Hz, 12H; $\text{C}_6\text{H}_3\{\text{CH}(\text{CH}_3)_2\}_2$). $^{13}\text{C}\{^1\text{H}\}$ NMR (125.80 MHz, CD_2Cl_2): δ (ppm) 146.0, 145.3 (*ortho*-Dipp); 144.2 (NCCHN); 137.2 (HCN_2); 133.9 (NCCHN); 133.1 ($\times 2$) (*para*-Dipp); 130.6, 129.6 (*ipso*-Dipp); 125.5 ($\times 2$) (*meta*-Dipp); 29.6, 29.5 ($\text{C}_6\text{H}_3\{\text{CH}(\text{CH}_3)_2\}_2$); 27.1, 24.6, 24.5, 22.7 ($\text{C}_6\text{H}_3\{\text{CH}(\text{CH}_3)_2\}_2$). ^1H NMR (500.30 MHz,

*d*₈-THF): δ (ppm) 9.58 (d, $^4J_{\text{H-H}} = 1$ Hz, 2H; *HCN*₂); 8.15 (d, $^4J_{\text{H-H}} = 1$ Hz, 2H; *NCCHN*); 7.68 (t, $^3J_{\text{H-H}} = 8$ Hz, 2H; *para*-Dipp); 7.61 (t, $^3J_{\text{H-H}} = 8$ Hz, 2H; *para*-Dipp); 7.51 (d, $^3J_{\text{H-H}} = 8$ Hz, 4H; *meta*-Dipp); 7.45 (d, $^3J_{\text{H-H}} = 8$ Hz, 4H; *meta*-Dipp); 2.88 (sept, $^3J_{\text{H-H}} = 7$ Hz, 4H; *C*₆H₃{*CH*(CH₃)₂})₂); 2.57 (sept, $^3J_{\text{H-H}} = 7$ Hz, 4H; *C*₆H₃{*CH*(CH₃)₂})₂); 1.41 (d, $^3J_{\text{H-H}} = 7$ Hz, 12H; *C*₆H₃{*CH*(CH₃)₂})₂); 1.24 (d, $^3J_{\text{H-H}} = 7$ Hz, 12H; *C*₆H₃{*CH*(CH₃)₂})₂); 1.22 (d, $^3J_{\text{H-H}} = 7$ Hz, 12H; *C*₆H₃{*CH*(CH₃)₂})₂); 1.11 (d, $^3J_{\text{H-H}} = 7$ Hz, 12H; *C*₆H₃{*CH*(CH₃)₂})₂). ¹³C{¹H} NMR (125.80 MHz, *d*₈-THF): δ (ppm) 147.2, 146.4 (*ortho*-Dipp); 143.9 (*NCCHN*); 140.6 (*HCN*₂); 134.2 (*NCCHN*); 133.5, 133.4 (*para*-Dipp); 131.8, 131.4 (*ipso*-Dipp); 126.0, 125.9 (*meta*-Dipp); 30.1, 30.0 (*C*₆H₃{*CH*(CH₃)₂})₂); 27.1, 24.9, 24.6, 23.1 (*C*₆H₃{*CH*(CH₃)₂})₂). ²⁷Al NMR (104.27 MHz, CD₂Cl₂): δ (ppm) 80.7 (s).

Synthesis of [(aIPr)₂SbBr][BAr^F₄]₂ ([10][BAr^F₄]₂). To a mixture of [(aIPr)₂SbBr₂]*Br* (143 mg, 0.126 mmol) and Na[BAr^F₄] (223 mg, 0.252 mmol) was added CH₂Cl₂ (5 mL) while stirring at ambient temperature to afford a colourless solution and precipitate followed by THF (5 mL). The solution was stirred for one hour then filtered and the solution layered with hexane to afford a colourless oil. Crystals suitable for single crystal X-ray diffraction spontaneously formed from the oil after standing for one month. (268 mg, 76% yield). Anal. Calcd for C₁₁₈H₉₆B₂Br₂F₄₈N₄Sb (2785.17): C 50.89%, H 4.47%, N 2.01%. Anal. Calcd for C₁₃₄H₁₂₈B₂Br₂F₄₈N₄O₄Sb (3073.59): C 53.36%, H 4.20%, N 1.82%. Found: C 53.30%, H 4.26%, N 1.78%. ESI-MS, positive ion mode (CH₂Cl₂, 60 °C, 4.5 kV): *m/z* 489.2186 (100%) [(aIPr)₂SbBr]²⁺ (Calcd 489.1976). ¹H NMR (500.30 MHz, CD₂Cl₂): δ (ppm) 8.62 (s, $^4J_{\text{H-H}} = 1$ Hz, 2H; *HCN*₂); 7.73 (m, 20H; BC(*CH*)₂(CCF₃)₂CH and *para*-Dipp and *NCCHN*); 7.68 (t, $^3J_{\text{H-H}} = 8$ Hz, 2H; *para*-Dipp); 7.56 (s, 8H; BC(*CH*)₂(CCF₃)₂CH); 7.50 (dd, $^3J_{\text{H-H}} = 8$ Hz, $^4J_{\text{H-H}} = 1$ Hz, 2H; *meta*-Dipp); 7.45 (dd, $^3J_{\text{H-H}} = 8$ Hz, $^4J_{\text{H-H}} = 1$ Hz, 2H; *meta*-Dipp); 7.44 (dd, $^3J_{\text{H-H}} = 8$ Hz, $^4J_{\text{H-H}} = 1$ Hz, 2H; *meta*-Dipp); 7.42 (dd, $^3J_{\text{H-H}} = 8$ Hz, $^4J_{\text{H-H}} =$

1 Hz, 2H; *meta*-Dipp); 2.27 (sept, $^3J_{\text{H-H}} = 7$ Hz, 2H; $\text{C}_6\text{H}_3\{\text{CH}(\text{CH}_3)_2\}_2$); 2.24 (sept, $^3J_{\text{H-H}} = 7$ Hz, 2H; $\text{C}_6\text{H}_3\{\text{CH}(\text{CH}_3)_2\}_2$); 2.18 (sept, $^3J_{\text{H-H}} = 7$ Hz, 2H; $\text{C}_6\text{H}_3\{\text{CH}(\text{CH}_3)_2\}_2$); 2.11 (sept, $^3J_{\text{H-H}} = 7$ Hz, 2H; $\text{C}_6\text{H}_3\{\text{CH}(\text{CH}_3)_2\}_2$); 1.35 (d, $^3J_{\text{H-H}} = 7$ Hz, 6H; $\text{C}_6\text{H}_3\{\text{CH}(\text{CH}_3)_2\}_2$); 1.23 (d, $^3J_{\text{H-H}} = 7$ Hz, 6H; $\text{C}_6\text{H}_3\{\text{CH}(\text{CH}_3)_2\}_2$); 1.21 (d, $^3J_{\text{H-H}} = 7$ Hz, 6H; $\text{C}_6\text{H}_3\{\text{CH}(\text{CH}_3)_2\}_2$); 1.18 (d, $^3J_{\text{H-H}} = 7$ Hz, 6H; $\text{C}_6\text{H}_3\{\text{CH}(\text{CH}_3)_2\}_2$); 1.16 (d, $^3J_{\text{H-H}} = 7$ Hz, 6H; $\text{C}_6\text{H}_3\{\text{CH}(\text{CH}_3)_2\}_2$); 1.15 (d, $^3J_{\text{H-H}} = 7$ Hz, 6H; $\text{C}_6\text{H}_3\{\text{CH}(\text{CH}_3)_2\}_2$); 1.14 (d, $^3J_{\text{H-H}} = 7$ Hz, 6H; $\text{C}_6\text{H}_3\{\text{CH}(\text{CH}_3)_2\}_2$); 1.05 (d, $^3J_{\text{H-H}} = 7$ Hz, 6H; $\text{C}_6\text{H}_3\{\text{CH}(\text{CH}_3)_2\}_2$). $^{13}\text{C}\{^1\text{H}\}$ NMR (125.80 MHz, CD_2Cl_2): δ (ppm) 162.2 (m, $^1J_{^{13}\text{C}-^{11}\text{B}} = 50$ Hz, $^1J_{^{13}\text{C}-^{10}\text{B}} = 17$ Hz; $\text{BC}(\text{CH})_2(\text{CCF}_3)_2\text{CH}$); 145.7, 145.1, 144.4, 144.1 (*ortho*-Dipp); 140.9 (HCN_2); 135.7 (NCCHN); 135.4 (NCCHN); 135.3 ($\text{BC}(\text{CH})_2(\text{CCF}_3)_2\text{CH}$); 134.5, 134.3 (*para*-Dipp); 129.3 (qq, $^2J_{^{13}\text{C}-^{19}\text{F}} = 31$ Hz, $^4J_{^{13}\text{C}-^{19}\text{F}} = 2$ Hz; $\text{BC}(\text{CH})_2(\text{CCF}_3)_2\text{CH}$); 128.6 ($\times 2$) (*ipso*-Dipp); 127.3, 126.6, 126.4, 126.0 (*meta*-Dipp); 125.1 (q, $^1J_{^{13}\text{C}-^{19}\text{F}} = 271$ Hz; $\text{BC}(\text{CH})_2(\text{CCF}_3)_2\text{CH}$); 117.9 (sept, $^3J_{^{13}\text{C}-^{19}\text{F}} = 4$ Hz; $\text{BC}(\text{CH})_2(\text{CCF}_3)_2\text{CH}$); 30.3, 30.2, 30.1, 30.0 ($\text{C}_6\text{H}_3\{\text{CH}(\text{CH}_3)_2\}_2$); 26.5, 25.4, 24.7, 24.4, 24.2, 23.9, 23.3, 22.7 ($\text{C}_6\text{H}_3\{\text{CH}(\text{CH}_3)_2\}_2$).

4.3. Analytical techniques.

Single crystal X-ray diffraction data were collected using either an Oxford Diffraction Supernova dual-source diffractometer equipped with a 135 mm Atlas CCD area detector or an Enraf-Nonius kappa-CCD diffractometer equipped with a 95 mm CCD area detector. Crystals were selected under Paratone-N[®] oil, mounted on micromount loops, and quench-cooled using an Oxford Cryosystems open flow N₂ cooling device. Data were collected at 150 K using mirror monochromated Cu K α radiation ($\lambda = 1.54184$ Å; Oxford Diffraction Supernova) or graphite-monochromated Mo K α radiation ($\lambda = 0.71073$ Å; Enraf-Nonius kappa-CCD). Data collected on the Oxford Diffraction Supernova diffractometer were processed using the CrysAlisPro package, including unit cell parameter refinement and interframe scaling (which was carried out using SCALE3 ABSPACK within CrysAlisPro).^[42] Equivalent reflections were merged, and diffraction patterns processed with the CrysAlisPro suite. For data collected on the Enraf-Nonius kappa-CCD diffractometer, equivalent reflections were merged and the diffraction patterns processed with the DENZO and SCALEPACK programs.^[43] Structures were subsequently solved using direct methods or using the charge flipping algorithm as implemented in the program SUPERFLIP,^[44] and refined on F^2 using the SHELXL-2013 package.^[45–47]

NMR samples were prepared inside a glovebox under nitrogen in NMR tubes equipped with a gas-tight valve. ¹H, ¹¹B, ¹³C{¹H}, ¹⁹F and ²⁷Al NMR spectra were acquired on a Bruker AVII or AVIII 500 MHz NMR spectrometer at 298 K. ¹H and ¹³C{¹H} NMR spectra are reported relative to tetramethylsilane (TMS) and were referenced to the most downfield residual solvent resonance (CD₂Cl₂: δ_H 5.32 ppm, δ_C 53.8 ppm; *d*₈-THF: δ_H 3.58 ppm, δ_C 67.6 ppm). ¹¹B, ¹⁹F, ²³Na and ²⁷Al NMR spectra were externally referenced to Et₂O·BF₃, CFCl₃,

NaCl and Al(NO₃)₃ in D₂O, respectively. Assignments of individual resonances was achieved using two-dimensional NMR techniques (HSQC and HMBC) where necessary.

Positive ion mode electrospray mass spectra were recorded on a Bruker MicrOTOF mass spectrometer. The samples (10–20 μM) were prepared inside a glovebox under argon and the sample injected through a standard PEEK tubing feedthrough directly to the mass analyser at 10 μL·min⁻¹.^[48]

Elemental analyses were performed by Elemental Microanalysis Ltd, Devon. 10–15 mg samples were sent in sealed, evacuated Pyrex ampoules. All values are an average of at least two data collections.

5. Acknowledgements

We thank the EPSRC, the University of Oxford and Christ Church College for financial support of this research (DTA studentship J.B.W.). We also thank the University of Oxford for access to Chemical Crystallography facilities and Elemental Microanalysis (Devon) for performing the elemental analyses. We also acknowledge the use of the University of Oxford Advanced Research Computing (ARC) facility in carrying out this work (<http://dx.doi.org/10.5281/zenodo.22558>).

6. Electronic Supplementary Information

CCDC 1560210–1560220 contain the supplementary crystallographic data for this paper (www.ccdc.cam.ac.uk/data_request/cif). Experimental details, NMR spectra, ESI-MS spectra and computational details are also available.

7. References

- [1] Bourissou, D.; Guerret, O.; Gabbai, F. P.; Bertrand, G. *Chem. Rev.* **2009**, *100*, 39–92.
- [2] Bertrand G. *Carbene Chemistry: From Fleeting Intermediates to Powerful Reagents*; Marcel Dekker: New York, 2002.
- [3] Herrmann, W. A. *Angew. Chem. Int. Ed.* **2002**, *41*, 1290–1309.
- [4] Glorius F. *N-Heterocyclic Carbenes in Transition Metal Catalysis (Topics in Organometallic Chemistry 21)*; Springer-Verlag: Berlin-Heidelberg, Germany, 2006.
- [5] Nolan S. P. *N-Heterocyclic Carbenes in Synthesis*; Wiley-VCH: Weinheim, Germany, 2006.
- [6] Díez-González, S.; Nolan, S. P. *Coord. Chem. Rev.* **2007**, *251*, 874–883.
- [7] Hahn, F. E.; Jahnke, M. C. *Angew. Chem. Int. Ed.* **2008**, *47*, 3122–3172.
- [8] Jacobsen, H.; Correa, A.; Poater, A.; Costabile, C.; Cavallo, L. *Coord. Chem. Rev.* **2009**, *253*, 687–703.
- [9] Díez-González, S.; Marion, N.; Nolan, S. P. *Chem. Rev.* **2009**, *109*, 3612–3676.
- [10] Mercks, L.; Albrecht, M. *Chem. Soc. Rev.* **2010**, *39*, 1903–1912.
- [11] Díez-González, S. *N-Heterocyclic Carbenes: From Laboratory Curiosities to Effective Synthetic Tools*; RSC Publishing: Cambridge, 2010.
- [12] The first isolated N-heterocyclic carbene was reported in: Arduengo III, A. J.; Harlow, R. L.; Kline, M. *J. Am. Chem. Soc.* **1991**, *113*, 361–363.
- [13] For selected reviews see: (a) Arnold, P. L.; Pearson, S. *Coord. Chem. Rev.* **2007**, *251*, 596–609; (b) Albrecht, M. *Chem. Commun.* **2008**, 3601–3610; (c) Schuster, O.; Yang, L.; Raubenheimer, H. G.; Albrecht, M. *Chem. Rev.* **2009**, *109*, 3445–3478; (d) Crabtree, R. H. *Coord. Chem. Rev.* **2013**, *257*, 755–766.
- [14] Braunschweig, H.; Dewhurst, R. D.; Hammond, K.; Mies, J.; Radacki, K.; Vargas, A. *Science* **2012**, *336*, 1420–1422.

- [15] Böhnke, J.; Braunschweig, H.; Constantinidis, P.; Dellerman, T.; Ewing, W. C.; Fischer, I.; Hammond, K.; Hupp, F.; Mies, J.; Schmitt, H.-C.; Vargas, A. *J. Am. Chem. Soc.* **2015**, *137*, 1766–1769.
- [16] Böhnke, J.; Braunschweig, H.; Dellerman, T.; Ewing, W. C.; Hammond, K.; Jimenez-Halla, J. O. C.; Kramer, T.; Mies, J.; *Angew. Chem. Int. Ed.* **2015**, *54*, 13801–13805.
- [17] Wang, Y.; Xie, Y.; Wei, P.; King, R. B.; Schaefer III, H. F.; Schleyer, P. v. R.; Robinson, G. H. *Science* **2008**, *321*, 1069–1071.
- [18] Sidiropoulos, A.; Jones, C.; Stasch, A.; Klein, S.; Frenking, G. *Angew. Chem. Int. Ed.* **2009**, *48*, 9701–9704.
- [19] Jones, C.; Sidiropoulos, A.; Holzmann, N.; Frenking, G.; Stasch, A. *Chem. Commun.* **2012**, *48*, 9855–9857.
- [20] Wang, Y.; Xie, Y.; Wei, P.; King, R. B.; Schaefer III, H. F.; Schleyer, P. v. R.; Robinson, G. H. *J. Am. Chem. Soc.* **2008**, *130*, 14970–14971.
- [21] Abraham, M. Y.; Wang, Y.; Xie, Y.; Wei, P.; Schaefer III, H. F.; Schleyer, P. v. R.; Robinson, G. H. *Chem. Eur. J.* **2010**, *16*, 432–435.
- [22] Böhnke, J.; Braunschweig, H.; Ewing, W. C.; Hörl, C.; Kramer, T.; Krummenacher, I.; Mies, J.; Vargas, A. *Angew. Chem. Int. Ed.* **2014**, *53*, 9082–9085.
- [23] Mondal, K. C.; Roy, S.; Dittrich, B.; Maity, B.; Dutta, S.; Koley, D.; Vasa, S. K.; Linser, R.; Dechert, S.; Roesky, H. W. *Chem. Sci.* **2015**, *6*, 5230–5234.
- [24] Back, O.; Kuchenbeiser, G.; Donnadiou, B.; Bertrand, G. *Angew. Chem. Int. Ed.* **2009**, *48*, 5530–5533.
- [25] Kretschmer, R.; Ruiz, D. A.; Moore, C. E.; Rheingold, A. L.; Bertrand, G. *Angew. Chem. Int. Ed.* **2014**, *53*, 8176–8179.
- [26] Waters, J. B.; Everitt, T. E.; Myers, W. K.; Goicoechea, J. M. *Chem. Sci.* **2016**, *7*, 6981–6987.

- [27] Berglund, M.; Wieser, M. E. *Pure Appl. Chem.* **2011**, *83*, 397–410.
- [28] Addison, A. W.; Rao, N. T.; Reedijk, J.; van Rijn, J.; Verschoor, G. C. *J. Chem. Soc., Dalton Trans.* **1984**, 1349–1356.
- [29] Cordero, B.; Gómez, V.; Platero-Prats, A. E.; Revés, M.; Echeverría, J.; Cremades, E.; Barragán, F.; Alvarez, S. *Dalton Trans.* **2008**, 2832–2838.
- [30] Batsanov, S. S. *Russ. Chem. Bull.* **1995**, *44*, 18–23.
- [31] Sidiropoulos, A.; Osborne, B.; Simonov, A. N.; Dange, D.; Bond, A. M.; Stasch, A.; Jones, C. *Dalton Trans.* **2014**, *43*, 14858–14846.
- [32] Green, M. L. H.; Parkin, G. *Dalton Trans.* **2016**, *45*, 18784–18795.
- [33] Aprile, A.; Corbo, R.; Tan, K. V.; Wilson, D. J. D.; Dutton, J. L. *Dalton Trans.* **2013**, *43*, 764–768.
- [34] Okuniewski, A.; Rosiak, D.; Chojnacki, J.; Becker, B. *Polyhedron*, **2015**, *90*, 47–57.
- [35] Breunig, H. J.; Denker, M.; Lork, E. Z. *Anorg. Allg. Chem.* **1999**, *625*, 117–120.
- [36] Althaus, H.; Breunig, H. J.; Lork, E. *Chem. Commun.* **1999**, 1971–1972.
- [37] Alič, B.; Štefančič, A.; Tavčar, G. *Dalton Trans.* **2017**, *46*, 3338–3346.
- [38] Kaya, S.; Kaya, C. *Inorg. Chem.* **2015**, *54*, 8207–8213.
- [39] Arduengo III, A. J.; Krafczyk, R.; Schmutzler, R.; Craig, H. A.; Goerlich, J. R.; Marshall, W. J.; Unverzagt, M. *Tetrahedron* **1999**, *55*, 14523–14534.
- [40] Jafarpour, L.; Stevens, E. D.; Nolan, S. P. *J. Organomet. Chem.* **2000**, *606*, 49–54.
- [41] Brookhart, M.; Grant, B.; Volpe, A. F. *Organometallics* **1992**, *11*, 3920–3922.
- [42] CrysAlisPro, Agilent Technologies, Versions 1.171.35.8 and 1.171.37.35.
- [43] Otwinowski, Z.; Minor, W. *Macromol. Crystallogr. Part A* **1997**, *276*, 307–326.
- [44] Palatinus, L.; Chapius, G. *J. Appl. Crystallogr.* **2007**, *40*, 786–790.
- [45] Sheldrick, G. M. *Acta Crystallogr. A* **1990**, *46*, 467–473.
- [46] Sheldrick, G. M. *Acta Crystallogr. A* **2008**, *64*, 112–122.

[47] Sheldrick, G. M. *SHELXL-2013, Programs for Crystal Structure Analysis* **2013**.

[48] Lubben, A. T.; McIndoe, J. S.; Weller, A. S. *Organometallics* **2008**, 27, 3303–3306.

TOC

